# Phylogenomic Analyses Reveal Hidden Diversity in *Gerrhonotus* (Anguidae: Gerrhonotinae) and Description of a New Species from Western Mexico

Adrián Nieto-Montes de Oca<sup>1</sup>, John J. Wiens<sup>2</sup>, and Uri Omar García Vázquez<sup>3,4</sup>

ABSTRACT: The genus Gerrhonotus has a wide geographic range, extending from Texas in the United States southward and eastward to Panamá. Despite this enormous distribution, only seven species are currently recognized within the genus. However, both morphological and molecular studies have provided evidence for the presence of an undescribed species in western Mexico that has historically been confused with G. liocephalus. This species remains undescribed. In addition, molecular studies have revealed significant genetic structuring within some of the most broadly distributed morphology-based species in the genus, including G. infernalis, G. liocephalus, and G. ophiurus. These findings suggest the potential for unrecognized species diversity. Here, we used double-digested restriction-site associated sequencing (ddRADseq) to construct a new phylogenomic data set for the genus Gerrhonotus. We performed maximum-likelihood analyses on concatenated matrices with varying minimum taxon coverage to assess the impact of different numbers of loci and proportions of missing data on matrix informativeness, and identified the optimal matrix. We then performed a maximum-likelihood analysis of this matrix. Based on the resulting tree, current taxonomy, and the geographic distribution of samples, we identified 10 potentially independent lineages (putative species) within the genus. Subsequently, we conducted species-tree analyses for these lineages and utilized the resulting topologies to estimate their genealogical divergence index (gdi), providing a preliminary assessment of their evolutionary distinctness. All of the analyses consistently corroborated the existence of an undescribed species from western Mexico. Moreover, gdi values indicated the potential presence of additional hidden species diversity within the genus. We describe the lineage from western Mexico as a distinct species, based on 18 adult specimens. The new species appears to be restricted to the western slopes of Mexico from southern Nayarit to central Guerrer

Key words: Alligator lizard; Biodiversity; Gerrhonotus; Phylogenomics; Species delimitation; Systematics; Taxonomy

Despite over two centuries of dedicated systematic research, the reptile diversity of Mexico remains incompletely known. Several dozen new squamate species from Mexico have been proposed for formal recognition in the last decade (Clause et al. 2020, and references therein). Some taxa, like the lizard genera Abronia and Xenosaurus, appear to be exceptions to an apparent decreasing rate of species discovery for the Mexican reptile fauna (Clause et al. 2020). The genus Gerrhonotus (Anguidae: Gerrhonotinae) is a relatively small genus composed of seven currently recognized species that collectively occur from Texas in the United States of America south and east through most of Mexico and Central America to Panamá (Good 1994; García-Vázquez et al. 2018a; Blair et al. 2022). This genus may soon represent another exception: two of these seven species have been described during the last two decades, another one is added herein, and additional species may yet be discovered (see the following).

Good (1994) performed a taxonomic review of the genus Gerrhonotus based on external morphology. This study led to the recognition of only four species: G. lugoi, G. infernalis, G. liocephalus, and G. ophiurus. However, the taxonomy of the genus has undergone significant modifications since then. On the one hand, molecular analyses found that G. lugoi is only distantly related to other species of Gerrhonotus (García-Vázquez et al. 2018a; Blair et al. 2022), and consequently it has been transferred to the new genus Desertum

(Blair et al. 2022). On the other hand, two species that were initially described as *Gerrhonotus* were subsequently transferred to other genera: *G. parvus*, described by Knight and Scudday (1985), was promptly relocated after its description to *Elgaria* by Smith (1986), but returned to *Gerrhonotus* 20 yr later by Conroy et al. (2005). Similarly, *G. rhombifer*, described by Peters (1876), was reclassified under the monotypic genus *Coloptychon* by Tihen (1949). It was later put back into *Gerrhonotus* by García-Vázquez et al. (2018a).

Additionally, three more species have been added to *Gerrhonotus* during the last two decades. The first was *G. farri*, described by Bryson and Graham (2010) from Tamaulipas. This was followed by *G. lazcanoi*, described by Banda-Leal et al. (2017) from Nuevo León. Shortly thereafter, *G. mccoyi* was described by García-Vázquez et al. (2018b) from Coahuila. Nonetheless, on the basis of its external morphology, *G. lazcanoi* also was recently transferred to the genus *Desertum* by Blair et al. (2022).

This expanded taxonomic knowledge does not necessarily imply that the systematics and taxonomy of the genus are fully resolved. In his taxonomic review, Good (1994) examined two small samples that were widely separated geographically in western Mexico from other populations of Gerrhonotus (his "western isolate populations"). One was composed of two specimens from Durango and one from Sinaloa (his Sample 19) and another was composed of one specimen from Colima and two from Jalisco (his Sample 20). These two samples shared some characters with G. liocephalus, but also differed from this taxon and from each other in several characters. Because of this variation and small

<sup>&</sup>lt;sup>1</sup> Laboratorio de Herpetología and Museo de Zoología "Alfonso L. Herrera", Departamento de Biología Evolutiva, Facultad de Ciencias, Universidad Nacional Autónoma de México, Ciudad Universitaria, Ciudad de México 04510, México

<sup>&</sup>lt;sup>2</sup> Department of Ecology and Evolutionary Biology, University of Arizona, Tucson, AZ 85721, USA

<sup>&</sup>lt;sup>3</sup> Laboratorio de Sistemática Molecular, Carrera de Biología, Unidad Multidisciplinaria de Investigación Experimental, Facultad de Estudios Superiores Zaragoza, Universidad Nacional Autónoma de México, Ciudad de México 09230, México

<sup>&</sup>lt;sup>4</sup> Correspondence: e-mail, urigarcia@gmail.com

sample sizes, Good (1994) was unable to find statistically significant differences in any character when he compared these isolates with other *Gerrhonotus* populations. Thus, he tentatively assigned them to *G. liocephalus*. Good (1994) also produced a phylogenetic hypothesis for the genus based on external morphology in which *G. ophiurus* was the sister taxon to a polytomy with *G. liocephalus* and his western isolate populations 19 and 20.

The western isolate population 19 of Good (1994) has not been further studied, and its taxonomic status remains uncertain. However, the other western population (20) has received more attention. Recently, Castiglia et al. (2010) performed a phylogenetic analysis (based mostly on sequences of the mitochondrial 16S rDNA and ND2 genes) that included samples of G. infernalis, G. liocephalus, G. parvus, and a specimen of Gerrhonotus from Chamela, Jalisco. They concluded that the latter specimen was very divergent from the other species of Gerrhonotus and that it probably represented an undescribed taxon. Later, García-Vázquez et al. (2018a) performed a phylogenetic analysis of Gerrhonotus based on the mitochondrial gene ND4. In this analysis, they included six samples from western Mexico: one from Colima, two from Jalisco, one from Nayarit, and two from Michoacán. These samples formed a strongly supported clade (the "G. western" clade) that was the sister taxon to a clade composed of G. liocephalus, G. infernalis, and G. ophiurus. However, this relationship was not strongly supported. The sister taxon to these two clades was G. rhombifer, and the sister taxon to all of these combined taxa was G. parvus. These last two relationships were strongly supported.

More recently, Blair et al. (2022) performed a phylogenetic analysis of *Gerrhonotus* based on 3157 UCE loci. In this analysis, they included two samples from the Pacific slopes of Jalisco and Michoacán. These samples formed a strongly supported "G. sp. western" clade, which was the sister taxon to a clade composed of G. liocephalus, G. infernalis, G. ophiurus, and G. rhombifer. The sister taxon to all these taxa was G. parvus. All of these relationships were strongly supported. Thus, the phylogenetic positions of "G. western" and G. rhombifer in the hypothesis of García-Vázquez et al. (2018a) were exchanged.

In summary, despite molecular evidence for a distinct lineage of *Gerrhonotus* in western Mexico (= "G. sp. Western" hereafter for simplicity), this lineage remains undescribed, and its phylogenetic position remains uncertain. Interestingly, during field work conducted on the Pacific Versant of Guerrero by one of us (UOGV) and his collaborators in the last few years, some previously unknown populations of *Gerrhonotus* were found that do not represent *G. liocephalus* and might belong to *G.* sp. Western instead.

In addition, recent systematic studies of *Gerrhonotus* have revealed additional problems in the systematics of the genus. Two species (*G. farri* and *G. rhombifer*) are known from very few specimens. Importantly, the first species has not been included in any molecular study to date. The taxonomic status of the older, more established taxa (*G. infernalis*, *G. liocephalus*, and *G. ophiurus*) has remained largely unchanged. However, some populations previously assigned to *G. infernalis* have been assigned to *G. mccoyi* (García-Vázquez et al. 2018b). This change rendered *G. infernalis* paraphyletic with respect to *G. mccoyi* in the molecular phylogenies by García-Vázquez et al. (2018a) and Blair et al.

(2022). The species *G. infernalis*, *G. liocephalus*, and *G. ophiurus* exhibit relatively large geographic distributions, occur in many habitats, and exhibit considerable population genetic structure (García-Vázquez et al. 2018a; Blair et al. 2022). This suggests that they may contain some hidden diversity within their taxonomic boundaries.

Herein, we perform a phylogenetic analysis of *Gerrhonotus* based on a newly generated double-digested, restriction site-associated DNA sequencing (ddRADseq) data set. We use these data to test the distinctness of the *G.* sp. Western lineage, reevaluate its phylogenetic position, determine whether previously unknown populations of *Gerrhonotus* on the Pacific Versant of Guerrero belong to this lineage, and conduct a preliminary assessment of potential hidden diversity within the genus.

## Materials and Methods Molecular Data

**Taxon sampling.**—We constructed a ddRADseq library for the genus *Gerrhonotus* including all available samples of G. infernalis (n = 20) and G. mccoyi (n = 4), as well as representatives of G. liocephalus (n = 5), G. ophiurus (n = 5), and G. parvus (n = 2). The G. sp. Western lineage, previously documented to occur only on the Pacific Versant of Mexico from Nayarit through southeastern Michoacán (Good 1994; Castiglia et al. 2010; García-Vázquez et al. 2018a,b; Blair et al. 2022), was represented by eight samples from Colima and Michoacán. In addition, we included six samples from previously undocumented populations in central Guerrero; their affinity with the G. sp. Western lineage remains uncertain. Outgroup taxa were selected based on the phylogenetic studies of García-Vázquez et al. (2018a) and Blair et al. (2022) and included representatives of two species of Abronia, and one species each of Barisia, Elgaria, and Desertum. For analyses involving outgroup taxa, Elgaria was used to root the trees (Pyron et al. 2013). Unfortunately, no tissue samples of G. rhombifer were available for this study. A complete list of the samples included in the analysis is given in Table 1, with the collection localities for most samples shown on the map in Fig. 1.

**Data collection.**—To sequence these samples, we used a modified version of the ddRADseq protocol of Peterson et al. (2012). High-molecular-weight DNA was extracted from liver or muscle tissue with the DNeasy Blood and Tissue kit (Qiagen, catalog number 69506). We assessed DNA quality on agarose gels (0.5%) and DNA concentration with a Qubit dsDNA Broad-Range Assay Kit (Invitrogen, catalog number Q32853) in a Qubit v2.0 fluorometer (Thermo Fisher Scientific). We double-digested 500 ng of genomic DNA per sample in a reaction of 20 µL with 20 units each of the common cutter MspI (restriction site 5'-CG-3', New England BioLabs [NEB], catalog number R0125S) and the rare cutter SbfI-HF (restriction site 5'-TGCA-3', NEB catalog number R3642S), in addition to the manufacturer-recommended buffer (rCutSmart Buffer, NEB). The reactions were incubated during 1 h and 40 min at 37°C, followed by SbfI-HF enzyme inactivation for 20 min at 80°C.

For dual indexing of samples, we employed the uniquely barcoded adapters and polymerase chain reaction (PCR) primers provided by Peterson et al. (2012). We first ligated barcoded adapters to each sample in a 30- $\mu$ L reaction with the P1 and P2 adapters, T4 DNA Ligase (NEB, Cat. No.

Table 1.—Locality information, number of raw reads obtained, and GenBank biosample accession numbers for samples used in this study. Abbreviations for institutional resource collections follow Sabaj (2023).<sup>a</sup>

Taxon	Institutional no.	Field no.	State	Locality	Latitude	Longitude	Elev.	Reads_raw	GenBank biosample accession no.
A. gadovii		UOGV827	Gro	Sierra de Malinaltepec, Ejido Tres Marías	17.12658	-98.69511		3231096	SAMN46188611
A. lythrochila	UMFS 1415		Chis	Teopisca	16.54345	-92.47597		1187763	SAMN46188589
B. imbricata		EPR1069	$_{ m c}$	Sierra de Alvarez; 2 km W Alvarez	22.03200	-100.61500		3302793	SAMN46188566
D. $lugoi$	MZFC-HE 23318	AMH345	Coah	Cuatrociénegas: Nueva Atalaya	26.79830	-102.14125		1406469	SAMN46188560
E. Kingu		AINMO4163	Non	Iecora	26.39361	-105.50554		020/134	SAIMIN40100505 CAMMAG100E64
G. infernalis		Ausun1 TH 9350	X Ł	Austin Crookett	31 09485	-96.7877		95756	SAMIN40100304 SAMN46188581
G. infernalis	TNHCH 25964	000	Ϋ́	Austin	30.06955	-98.09258		254930	SAMN46188582
G. infernalis		CIG1809	N	La Ascención-La Escondida	24.24615	-99.86476		2486604	SAMN46188565
G. infernalis	<b>MZFC-HE 7465</b>	JJW393	NF	La Poza	26.27084	-100.09582		925226	SAMN46188572
G. infernalis	UANL 6345		NF	Chipinque	25.61403	-100.35417		890896	SAMN46188584
G. infernalis		UOGV4272	NF	Sierra de Gomas	26.36472	-100.49234		3682760	SAMN46188605
G. infernalis		UOGV548	NF	Rancho El Manzano; Santiago-Laguna	25.35233	-100.19350		51935	SAMN46188610
		0010074144	(	Santiago road	100	00000		001000	10100101101010
G. infernalis		ANMO2189 DWD7406	Coap	Iorreon, Sierra de Jimulco Sierra I e Concombia	25.18117	-103.29303		822123	SAMIN46188561 CAMM46188570
G. infernalis		RWB7407	Coall	Sierra La Concordia Sierra La Concordia	28.02422 98.09499	-103.01090		1409867	SAMIN40100279 SAMN46188580
G. infernalis		UOGV1393	Coah	Sierra de Iimulco	25.18117	-103.29303		895914	SAMN46188590
G. infernalis	MZFZ 5019	UOGV3690	Dgo	Santiago Papasquiaro	25.08525	-105.54134		290772	SAMN46188603
G. infernalis	MZFZ 5020	UOGV3691	Dgo	Santiago Papasquiaro	25.08525	-105.54134		2771992	SAMN46188604
G. infernalis		PPND	Gto	Sierra Gorda	21.73339	-101.07881		73111	SAMN46188577
G. infernalis		UOGV3503	Hgo	Zimapán	20.71997	-99.41203		1170242	SAMN46188595
G. infernalis	MZFC-HE 7825	FMQ3044	Qro	Sierra Gorda	20.69333	-99.54000		625548	SAMN46188568
G. infernalis	MZFC-HE 8013	FMQ3098	Qro	Sierra Gorda	20.69056	-99.53611		328334	SAMN46188569
G. infernalis	MZFC-HE 33392	KWB0239	SLP	Las Lagunas	22.72398	-100.38/00		8010105	SAMIN46188578
G. infernalis	UAINL 6782		SLF	5 mi E San Francisco, Valle de los Fontamos	22.06586	-100.01924		574497	SAMIN46188387
C hocenhalus	MZEC.HF 33390	A NIMO3919	Vo.	Fantasmas Cerro Baúl	16 54833	-94 17333		66359	SAMM46188569
G. liocephalus	MZFC-HE 16988	IAC23140	Oax	Sierra Mixe: Santa María Guienagati	16.74373	-95.45294		1876800	SAMN46188570
G. liocephalus	MZFC-HF 20366	IAC25255	Gro	Vallectios	17.97612	-101.62099		48026	SAMN46188571
G. liocephalus		NDAfricam	Pue	Africam Safari	18.93355	-98.13645		503799	SAMN46188575
G. liocephalus		UOGV4505	Gro	Las Fundiciones	17.46981	-100.27592		875897	SAMN46188608
G. mccóyi		UOGV1438	Coah	Cuatrociénegas: Churince	26.84175	-102.13608		2771566	SAMN46188591
G. mccoyi	MZFC-HE 29652	UOGV2055	Coah	Cuatrociénegas: Churince	26.84175	-102.13608		3069485	SAMN46188592
G. mccoyi	$MZFC-HE\ 29654$	UOGV2057	Coah	Cuatrociénegas: Churince	26.84175	-102.13608		764600	SAMN46188593
G. mccoyi		UOGV2077	Coah	Cuatrociénegas: Pozas Azules	26.82581	-102.02247		356372	SAMN46188594
G. ophiurus	MZFC-HE 7824	FMQ3041	$_{ m Hgo}$	Zoquizoquiapan	20.66028	-98.72583		6419973	SAMN46188567
G. ophiurus		Chapulhuacán	Hgo	Chapulhuacán	21.15867	-98.91756		1714193	SAMN46188576
G. ophiurus	UANL 6783		SLP	15 mi E de San Francisco	22.05400	-100.37785		2371583	SAMN46188588
G. ophiurus	UANL 45		Tams	Gómez Farías	23.02239	-99.14685		53197	SAMN46188583
G. ophurus	MZFC-HE 13879		ver.	Los Tuxtias	18.43304	10000001		323911	SAMIN46188574 CAMMA6188585
G. parous	UAINE 6621			Canon San Isiaro	25.55540	-100.52521		1001/94	SAIMIN40100303
G. parous	MZEZ 4948	A EVR190	] [ ] [	Canon San Isiaro Minetitlán: Mine Boão Colonodo	10.35078	-100.52521 104.07547	908	1632266	SAMM46199557
	MZFZ 4949	AEVB121	<u> </u>	Minatitlán: Mina Peña Colorada Minatitlán: Mina Peña Colorada	19.35978	-104.07547	85.6	1004250	SAMN46188558
G. sp. Western	MZFZ 5018	AEVB122	Col	Minatitlán: Mina Peña Colorada	19.35853	-104.07823	747	5028299	SAMN46188559
G. sp. Western <sup>M</sup>	MZFC-HE 14110	ANMO526	Mich	Chinicuila: near Puerto del Caimán	18.67745	-103.40713	1340	1069121	SAMN46188573
G. sp. Western	MZFZ 4950	UOGV3645	Col	Minatitlán: Cerro Moreno	19.35793	-104.11960	938	416602	SAMN46188596
G. sp. Western	MZFZ 4951	UOGV3646	Col	Minatitlán: Cerro Moreno	19.35793	-104.11960	938	4530404	SAMN46188597
G. sp. Western	MZFZ 4952	UOGV3647	Col	Minatitlán: Cerro Moreno	19.35793	-104.11960	938	5866282	SAMN46188598

Table 1.—Continued.

Taxon	Institutional no.	Field no.	State	Locality	Latitude	Longitude	Elev.	Reads_raw	GenBank biosample accession no.
G. sp. Western	MZFZ 4953	UOGV3648	Col	Minatitlán: Cerro Moreno	19.35793	-104.11960	938	3727181	SAMN46188599
G. sp. Western	MZFZ 4954	OGV3650	Gro	Puerto El Edén	17.46835	-100.74510	1500	550115	SAMN46188600
G. sp. Western	MZFZ 4955	UOGV3651	Gro	Puerto El Edén	17.46835	-100.74510	1500	104423	SAMN46188601
G. sp. Western*	MZFZ 4956	UOGV3653	Gro	Puerto El Edén	17.46835	-100.74510	1500	1693853	SAMN46188602
G. sp. Western	MZFZ 4957	UOGV4503	Gro	Atoyac de Álvarez: La Florida	17.21944	-100.36889	810	1778256	SAMN46188606
G. sp. Western	MZFZ 4958	UOGV4504	Gro	Atoyac de Álvarez: La Florida	17.21944	-100.36889	810	7732033	SAMN46188607
G. sp. Western	MZFZ 4959	UOGV4506	Gro	Atoyac de Álvarez: La Florida	17.21944	-100.36889	810	478251	SAMN46188609
G. sp. Western	MZFC-HE 8038	ALC 626	Col	Km 1.5 camino al Terrero	19.42917	-103.94056	1110	No	Not sequenced
G. sp. Western <sup>M,U</sup>	MZFC-HE 32963	ANMO1167	Col	Approx. 1.4–2.4 km E La Central	19.14900	-104.42647	44	No	Not sequenced
$G. \text{ sp. Western}^{M}$	MZFC-HE 8428	FSLG001	[a]	Puerto Los Mazos, Manantlán (cerca de	19.68833	-104.39528	2500	No	Not sequenced
1				torre de microondas)					•
G. sp. Western <sup>M</sup>	MZFC-HE 32964	ACMX 14	[a]	Chamela	19.52678	-105.07381		No	Not sequenced
$G. \text{ sp. Western}^{M,U}$	MZFC-HE 32965	ANMO1097	Mich	El Taguazal, approx. 25 km por carr de	18.23392	-102.24733	757	No	Not sequenced
:				Arteaga hacia Playa Azul					ı
$G. \text{ sp. Western}^{M*}$		ISZ665	Nay	Mesillas, Compostela	21.22268	-105.01430	446	No	Not sequenced

= Coahuila; Col = Colima; Dgo = Durango; Gro = Guerrero; Gto = Guanajuato; = San Luis Potosí; Son = Sonora; Tams = Tamaulipas; TX = Texas; Ver = Veracruz. For the G. sp. Western lineage, superscripts M and U indicate samples sequenced for mitochondrial data (García-Vázquez et al. 2018a) and UCE data (Blair et al. 2022), respectively, and the asterisks denote specimens unavailable for morphological examination. ANMO, CIG, EPR, ISZ, PPND, RWB, TJL, and UOGV are field collector abbreviations for specimens pending to be catalogued at the MZFG-HE or MZFZ Hgo = Hidalgo; [al = Jalisco; Mich = Michoacán; Nay = Nayarit; NL = Nuevo León; Oax = Oaxaca; Pue = Puebla; Qro = Querétaro; SLP

M0202S), and the recommended buffer (T4 DNA Ligase Reaction Buffer, NEB). We incubated the reactions for 40 min at 20°C, followed by heat inactivation of the ligase during 20 min at 80°C.

Ligated samples with unique adapter barcodes were then pooled and cleaned with 1.5x magnetic carboxylate beads (SpeedBeads, SIGMA Cat. No. GE6515210505025). Pools were subsequently size selected (470–630 bp) with a Pippin Prep (Sage Science, SW v6.40) and amplified with Phusion High-Fidelity DNA polymerase and uniquely barcoded PCR primers. The following amplification protocol was used: (a) 98°C for 30 s, (b) 98°C for 10 s, (c) 65°C for 30 s, (d) 72°C for 30 s, (e) eight cycles of steps (b–d) and (f) 72°C for 10 min. Following another cleanup and pooling, pools were quantified using an Agilent Bioanalyzer (Agilent 2100) at Centro de Investigaciones y de Estudios Avanzados (Cinvestav), Instituto Politécnico Nacional. Finally, the ddRAD-seq library was sent to Macrogen Korea laboratories for sequencing in an Illumina HiSeqX (150PE) lane.

Bioinformatics.—We evaluated the quality of raw Illumina reads with FastQC (v0.11.5; Andrews 2010), and then used the pipeline ipyrad (v0.9.50; Eaton and Overcast 2020) to process the ddRADseq data. This pipeline performs a de novo clustering using VSEARCH (v2.15.0; Rognes et al. 2016) and aligns the resulting clusters with MUSCLE (v3.8.31; Edgar 2004). To complete assemblies in ipyrad, we used default settings for all parameters except for the following: maximum number of barcode mismatches = 1 (because all adapter barcodes used differed by at minimum two base positions, which is sufficient to achieve >95%-99% assignment of individual reads; Peterson et al. 2012); filter adapters = 2 (strict, to trim all Illumina adapters and barcodes); minimum depth at which statistical and majority rule base calls are made during consensus base calling = 10 each, and clustering threshold = 0.95. To estimate a clustering threshold (CT) that minimizes false homozygosity and heterozygosity (optimal CT), we previously generated assemblies in ipyrad at eight different CT values (set at increments of 0.2 between 0.84 and 0.98), and then evaluated the following four metrics based on population and landscape genetics proposed by McCartney-Melstad et al. (2019): (1) the fraction of inferred paralogous clusters; (2) heterozygosity; (3) total number of single nucleotide polymorphism (SNPs) recovered; and (4) the fraction of variance explained by the main principal components of genetic variation.

Phylogenetic inference.—To infer the phylogenetic relationships of Gerrhonotus, we first performed maximum likelihood (ML) analyses of the concatenated loci. To explore the effect on phylogenetic inference of varying numbers of loci and proportions of missing data, we first used ipyrad to generate different alignment matrices with increments of ~10% in minimum-taxon coverage (MTC, the minimum number of samples that must have data for a locus to be included in the matrix). These ranged from  $\sim 10\%$  to ~70% of the samples (i.e., MTC10, MTC20...MTC70 matrices). We then performed ML analyses of these matrices with RAxML (v8.2.12; Stamatakis 2014). The matrices included all concatenated loci, and included both SNPs and invariant sites to improve estimation of branch lengths and topology (Leaché et al. 2015). For each matrix, we performed 1000 rapid bootstrap inferences and subsequent search for the best-scoring ML tree, with the GTR + GAMMA model and starting from

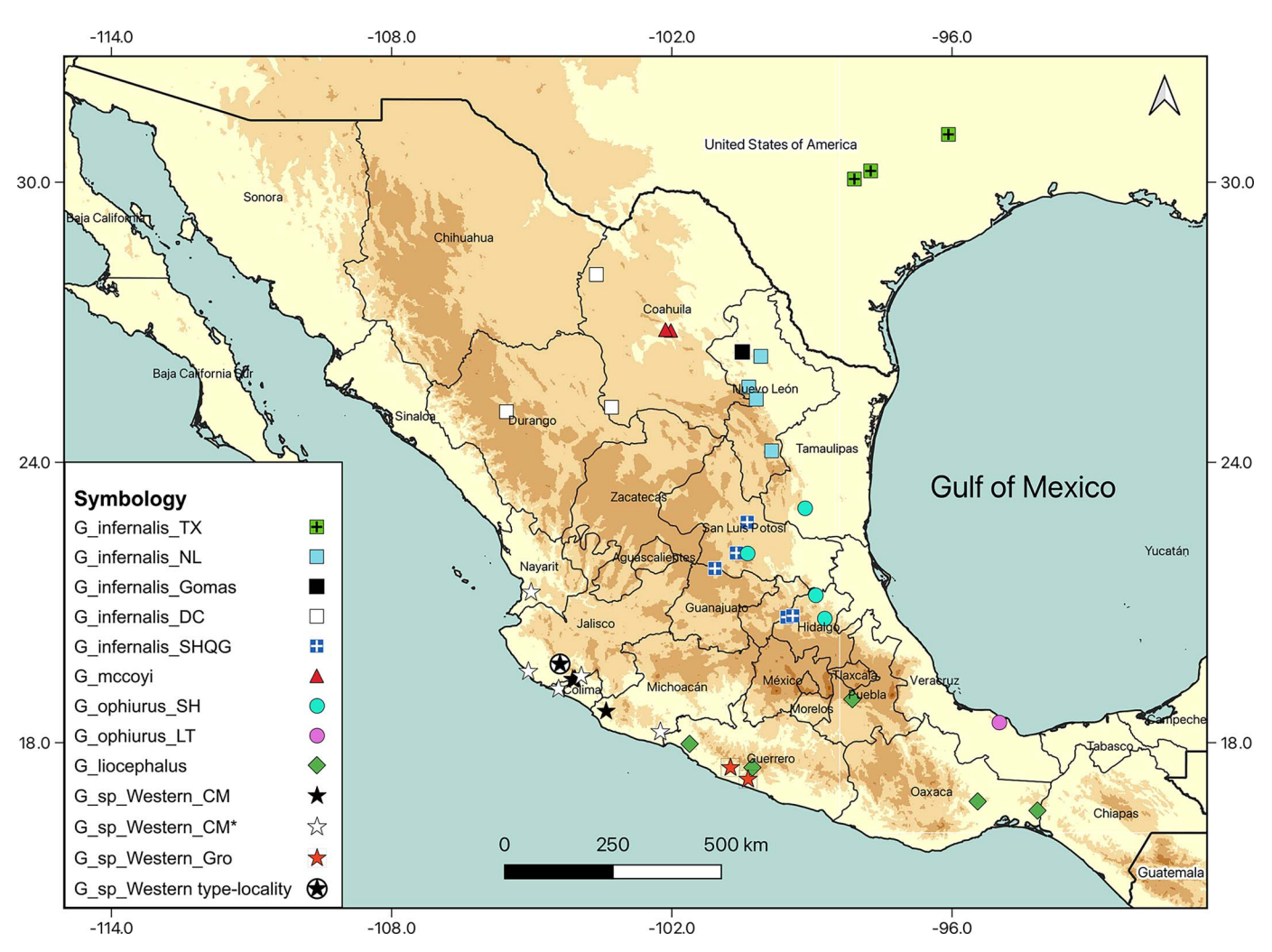


Fig. 1.—Localities for lizards in the genus *Gerrhonotus* (exclusive of *G. parvus*) sampled for this study. Also shown are collecting localities of specimens of *G.* sp. Western that were only included in the morphological analysis and/or included in other molecular phylogenetic studies (*G.* sp. Western\_CM\*). Sublineages of *G. infernalis*, *G. ophiurus*, and *G.* sp. Western are potentially independent evolutionary lineages evaluated in the species delimitation analyses. A color version of this figure is available online.

random-addition-sequence trees. We performed analyses on the Mana high-performing computing cluster of the University of Hawaii. We used FigTree (v1.4.4; Rambaut 2018) to visualize trees. The matrix yielding the highest proportion of well-supported nodes (bootstrap values  $\geq 70\%$ ) was selected as the matrix with the optimal MTC or optimal matrix.

In the concatenated tree inferred from the optimal matrix (see Results), G. infernalis was strongly supported as paraphyletic with respect to both G. mccoyi and G. ophiurus. In addition, substantial genetic structure was observed within G. infernalis, G. ophiurus, and an expanded G. sp. Western clade, which now included the previously undocumented lineage from Guerrero. As in previous studies (García-Vázquez et al. 2018a; Blair et al. 2022), this genetic structure suggested the potential presence of hidden diversity in the genus. To investigate this potential hidden diversity, we initially identified potentially independent lineages based on the concatenated tree, current taxonomy, and the geographic distribution of samples. Subsequently, we conducted speciestree analyses that incorporated both lineages considered clearly independent (G. liocephalus and G. parvus) and those regarded as potentially independent (see the following).

Finally, the resulting species trees were used as guide trees for estimating the genealogical divergence index between populations, providing a preliminary assessment of the distinctness of all identified lineages (see below).

Species trees.—In addition to *G. mccoyi*, we identified the following nine lineages as potentially independent: within *G. infernalis*, the clades from Texas (*G. infernalis*\_TX), Nuevo León (*G. infernalis*\_NL), Durango and Coahuila (*G. infernalis*\_DC), and San Luis Potosí, Hidalgo, Querétaro, and Guanajuato (*G. infernalis*\_SHQG), along with the sample from the Sierra de Gomas, Nuevo León (*G. infernalis*\_Gomas); within *G. ophiurus*, the clade from Hidalgo, San Luis Potosí, and Tamaulipas (*G. ophiurus*\_SH) and the sample from Los Tuxtlas, Veracruz (*G. ophiurus*\_LT), and within the *G.* sp. Western lineage, the clades from Colima and Michoacán (*G.* sp. Western\_CM) and Guerrero (*G.* sp. Western\_Gro). Including *G. liocephalus* and *G. parvus*, this resulted in a total of 12 lineages in the analysis.

We conducted three distinct species-tree analyses of these lineages under the multispecies coalescent model. We first generated an alignment in ipyrad with the same parameters as the MTC10 matrix, except that MTC was adjusted to retain only loci with data from at least 80% of the samples. With some exceptions (see the following), we also excluded samples that had data for less than 70% of the loci. The resulting alignment was then used to conduct an A01 analysis in Bayesian phylogenetics and phylogeography (BPP; v4.7; Yang 2015; Flouri et al. 2018) to estimate a species tree. The analysis was based on 574 loci and was run for  $1 \times 10^6$  iterations, with a burn-in of 20,000 iterations and a sample frequency of 10. We assigned the population size parameters ( $\theta$ s) the inverse-gamma prior IG (3, 0.003), with mean of 0.0015, on the basis of the mean uncorrected pairwise genetic distance (p-distance) within the taxa. The divergence time at the root of the tree (t0) was assigned an inverse-gamma prior IG (3, 0.034), with mean 0.017, based on the mean p-distance between the basal-most taxon (G. parvus) and the other taxa. The remaining divergence-time parameters were specified by the uniform Dirichlet distribution (Yang and Rannala 2010). We used the concatenated tree topology as the starting tree. The analysis was run four times to confirm consistency across runs.

We also conducted a species-tree analysis using SVDquartets (Chifman and Kubatko 2014) in PAUP (v4.0a; Swofford 2002). First, we generated an alignment of unlinked SNPs (one SNP per locus) using ipyrad, applying the same parameters as the MTC10 matrix but using a MTC of 5 to increase the number of characters included in the analysis. We performed exhaustive quartet sampling with a species-membership partition, the multispecies coalescent model, 100 bootstrap replicates, and default settings for other parameters.

Finally, we conducted a species-tree analysis using the SNAPP package in Beast2 (v2.7.7; Bouckaert et al. 2019) with the same alignment of unlinked SNPs used in the BPP analyses. Mutation rates u and v were set to 1.0. We enabled MCMC sampling of the coalescence rate, initializing the analysis with a starting value of 10. For the prior on lambda, we used a gamma distribution with an alpha shape parameter of 2 and a beta scale parameter to 357, as estimated from the concatenated tree. The initial value of lambda was set to 10. A gamma prior distribution was also used for theta, with an alpha shape parameter of 1 and a beta rate parameter of 322, corresponding to a prior mean on theta of 0.0031 as estimated by the BPP analysis. The chain length was set to  $2 \times 10^6$  generations, storing every 1000 samples. Convergence was assessed using Tracer (v1.7.2; Rambaut et al. 2021).

**Potential hidden diversity assessment.**—We used the heuristic criterion for species delimitation based on the genealogical divergence index (gdi) between populations, following the approach proposed by Leaché et al. (2019). This method employs thresholds derived from an empirical meta-analysis conducted by Jackson et al. (2017), which suggests that gdi values <0.2 suggest a single species, gdi values >0.7 suggest distinct species, and gdi values between 0.2 and 0.7 indicate ambiguous delimitation. Using this framework, we performed a preliminary assessment of the distinctness of the potentially independent lineages. We conducted A00 analyses in BPP using the same alignment as in the BPP species-tree analyses to estimate species divergence times and population sizes for the evaluated lineages under the multispecies coalescent model. Each species-tree topology from the previous species-tree analyses (see above) was used as a guide tree. We then estimated gdi values using the posterior means of these parameters (Leaché et al. 2019; their Equation 7). Each A00 analysis was based on 500 loci

and ran for 8,000,000 iterations, with a burn-in of 50,000 iterations and sampling frequency of 10. Priors for the population-size parameters ( $\theta$ s) and the root divergence time of the species tree (t0) were assigned as in the BPP species-tree analysis, and other divergence-time parameters were specified by the uniform Dirichlet distribution (Yang and Rannala 2010). We used Tracer (v1.7.2; Rambaut et al. 2021) to confirm chain stationarity and ensure that the effective sample size was above 200 for all parameters.

## Morphological Data

**Sampling.**—We examined a total of 18 specimens representing the Gerrhonotus sp. Western lineage (see Results). These specimens were collected over the past three decades through field work in the states of Jalisco, Colima, Michoacán, and Guerrero by herpetologists from the Museo de Zoología Alfonso L. Herrera, Facultad de Ciencias, Universidad Nacional Autónoma de México (MZFC-HE), or the Museo de Zoología, Facultad de Estudios Superiores Zaragoza, Universidad Nacional Autónoma de México (MZFZ), as well as by local collectors working with these herpetologists. The specimens were euthanized with sodium pentobarbital, fixed in 10% buffered formalin, and subsequently transferred to 70% ethyl alcohol for permanent storage. The specimens were deposited in the herpetological collections of the MZFC-HE or the MZFZ. In addition, for comparative purposes, we examined 25 specimens of G. liocephalus from the states of Chiapas, Mexico, Guerrero, Oaxaca, and Puebla (see Appendix).

We obtained ddRADseq data from 14 of the above 18 specimens of the G. sp. Western lineage (Table 1). García-Vázquez et al. (2108a) and Blair et al. (2022) also included five and two of them in their phylogenetic analyses based on mitochondrial and UCE data, respectively. A list of the specimens sequenced in these studies is provided in Table 1. Institutional abbreviations for museums and collections follow Sabaj (2023).

**Data.**—Scale nomenclature followed Good (1994) and García-Vázquez et al. (2018b). Scale counts were performed using a dissecting microscope. Measurements were taken with calipers to the nearest 0.1 mm. Head length was measured from the tip of the snout to the anterior margin of the ear. For characters examined on the left and right sides of each specimen, values are reported as left side/right side. Color codes used in the description of color pattern are those of Smithe (1981).

## RESULTS ddRADseq Libraries

A total of 102,344,315 R1 sequence reads were obtained from 55 ddRADseq libraries. The 50 samples of Gerrhonotus had a mean number of reads per sample of 1,798,969 (min = 48,026; max = 8,010,105; SD = 2,021,356). The number of raw reads obtained from each sample is given in Table 1. Based on the four estimated metrics for assessing optimal clustering thresholds in ddRADseq data (Supplemental Fig. S1, available online), we used a clustering threshold of 0.95 to build assemblies in ipyrad.

Table 2.—Statistics for matrices with different minimum percentages ( $\sim 10\%$ –70%) of samples that have data for their respective loci and proportion of strongly supported nodes in the ML phylogenetic trees for Gerrhonotus inferred from them. Matrix names indicate the minimum taxon coverage (MTC) or minimum percentage of samples that have data for their loci. Number of Pis = number of parsimony-informative sites in a matrix. The asterisk indicates optimal matrix determined by ML methods.

Name	Number of loci	Concatenated length (bp)	Missing data (%)	Number of Pis	Nodes with bootstrap ≥70 (%)	Nodes with bootstrap ≥90 (%)
MTC10*	32,213	4,345,853	73.7	95,775	86.96	82.61
MTC20	18,654	2,577,308	65.1	74,086	84.78	82.61
MTC30	11,341	1,584,434	57.9	51,344	82.61	78.26
MTC40	6355	894,005	51.1	31,180	86.96	76.09
MTC50	2793	394,906	43.6	14,610	86.96	76.09
MTC60	882	124,826	35.6	4699	82.61	73.91
MTC70	210	29,733	27.7	1225	71.74	60.87

## Phylogenetic Inference

The monophyly of Gerrhonotus was consistently and strongly supported across all concatenated trees (MTC ranging from  $\sim$ 10% to 60%), with G. parvus consistently placed as the sister taxon to a strongly supported clade comprising all other Gerrhonotus (Supplemental Fig. S2, available online). In the trees from the matrices with the highest (optimal matrix) and second-highest proportions of strongly supported nodes (MTC ~20% and  $\sim 10\%$ , with proportions of 86.8% and 83.0%, respectively), Abronia and Barisia formed a strongly supported clade that was weakly supported as the sister taxon to Gerrhonotus, whereas Desertum was weakly supported as the sister taxon to these combined clades (Fig. S2). Because investigating the relationships of Gerrhonotus to other genera is beyond the scope of this paper, subsequent analyses focused exclusively on Gerrhonotus, with G. parvus as the sole outgroup to all other Gerrhonotus. Consequently, ML analyses evaluating the effects of varying numbers of loci and missing data proportions were conducted again on a reduced data set, including only Gerrhonotus (Table 2).

These analyses (Table 2) showed that the highest proportion of strongly supported nodes was in the concatenated tree from the MTC10 matrix (proportion  $\geq$ 70% = 86.96%; proportion  $\geq 90\% = 82.61\%$ ). This matrix clearly had the most loci, longest concatenated length, and the most parsimony-informative sites, but also the most missing data. The MTC20 matrix had the same proportion of nodes with bootstrap values  $\geq 90\%$  (82.61%) as the MTC10 matrix, but a slightly lower proportion of nodes with bootstrap values  $\geq$ 70% (84.78%). Conversely, the MTC40 and MTC50 matrices also had high proportions of nodes with bootstrap values  $\geq$ 70% (86.96%) but somewhat lower proportions of nodes with bootstrap values  $\geq 90\%$  (76.09%) than MTC10 and MTC20 (82.61%). Overall, we regarded the MTC10 as the optimal matrix because of the high proportions of strongly supported nodes inferred from it and the maximum number of loci (32,213) and parsimony-informative sites (95,775).

In the concatenated ML tree based on the optimal matrix (Fig. 2), the *Gerrhonotus* samples (above *G. parvus*) grouped into two main clades. The first main clade contained *G. lioce-phalus* as the sister taxon to the *G.* sp. Western clade, which included the *G.* sp. Western\_Gro and *G.* sp. Western\_CM lineages. The second main clade comprised three distinct subclades. The first subclade contained *G. ophiurus*\_LT and *G. ophiurus*\_SH. The second subclade, sister to the first,

comprised *G. infernalis\_NL* and a lineage in which *G. infernalis\_Gomas* was the sister taxon to *G. infernalis\_TX* and *G. mccoyi*. The third subclade, sister to the first two, contained the remaining *G. infernalis* samples, comprising *G. infernalis\_DC* and *G. infernalis\_SHQG*. All clades and relationships were strongly supported. In general, these clades and subclades were recovered and strongly supported across the remaining concatenated trees.

## Species Trees

The ipyrad alignment used for the four replicates of the BPP species tree analysis included 574 loci with data for at least 30 out of 38 samples (~80% coverage). Most samples had data for over 70% of the loci. The alignment included 15 samples of G. infernalis (G. infernalis NL= 3; G. inferna $lis_TX = 2$ ; G.  $infernalis_DC = 6$ ; G.  $infernalis_SHQG = 3$ ;  $G. infernalis\_Gomas = 1)$ , two samples of G. liocephalus, three samples of G. mccoyi, four samples of G. ophiurus (G. ophiurus\_SH = 3; G. ophiurus\_LT = 1), one sample of G. parvus, and 14 samples of G. sp. Western (G. sp. West $ern_CM = 8$ ; G. sp. Western\_Gro = 6). Despite lower data coverage, we retained certain samples due to the limited number of representatives from some potentially independent lineages. These included one G. infernalis\_TX sample (TJL2350) with 37.6% locus coverage, one G. mccoyi sample (UOGV2077) with 51.2% coverage, and one G. ophiurus sample (MZFC13879) with 37.8% coverage. Additionally, we retained three samples of the G. sp. Western\_Gro lineage (UOGV3650, UOGV4503, and UOGV4504), each with 54%-62% locus coverage.

The estimated species trees were generally consistent across the four conducted replicates (Fig. 3A, B) but showed notable differences from the concatenated tree. First, unlike in the concatenated tree, the clade containing G. infernalis\_NL, G. infernalis\_Gomas, and G. infernalis\_TX, along with G. mccoyi, was not the sister taxon to G. ophiurus. Instead, it was consistently recovered as the sister taxon to G. infernalis\_DC and G. infernalis\_SHQG, with strong support in two replicates, nearly strong support (PP = 0.94) in one, and weak support in the other. Second, G. ophiurus\_SH and G. ophiurus\_LT formed a weakly supported clade in two replicates, whereas in the others, G. ophiurus\_SH was the sister taxon to the G. infernalis-G. mccoyi clade, also with weak support. Third, the clade of G. liocephalus and G. sp. Western was strongly supported in one replicate, but moderately supported (PP = 0.82-0.88) in the remaining three.

The SVDquartets analysis used the same sampling of potentially independent lineages as in the BPP analysis. It was conducted on an alignment of 30,298 unlinked SNPs. Exhaustive quartet sampling included 39,306 quartets. The total weight of compatible quartets was 396.26 (80.05%), while incompatible quartets had a total weight of 98.74 (19.95%). The resulting tree (Fig. 3C) showed the same topology as the concatenated tree, except that *G. infernalis\_Gomas* was not the sister taxon to *G. infernalis\_TX* and *G. mccoyi*. Instead, it was the sister taxon to *G. infernalis\_NL*. Also, the *Gerrhonotus* clade excluding *G. parvus*, the (*G. liocephalus + G.* sp. Western) clade, and the (*G. infernalis\_G. mccoyi + G. ophiurus*) clade were weakly supported.

The alignment of unlinked SNPs for the SNAPP analysis included 554 sites. The resulting species tree (Fig. 3D)

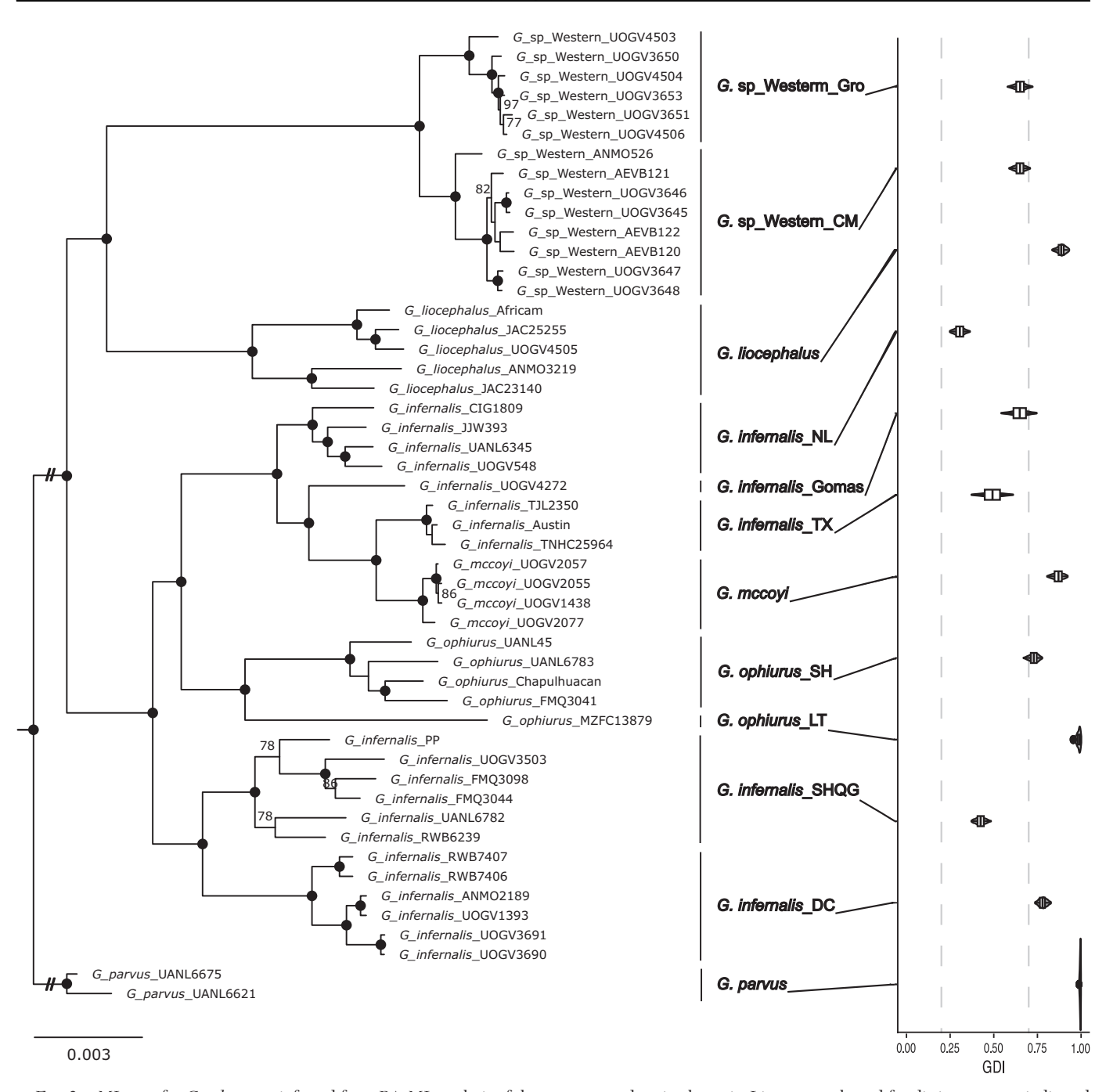


Fig. 2.—ML tree for *Gerrhonotus* inferred from RAxML analysis of the concatenated optimal matrix. Lineages evaluated for distinctness are indicated adjacent to the tree, with violin plots to their right illustrating the 95% credible interval for gdi estimates from BPP for each lineage. Filled black circles at nodes denote those in which the bootstrap support value = 100, and numbers above branches indicate bootstrap support values exceeding 70. The scale bar represents substitutions per site. The gdi estimates were calculated using the BPP species tree topology of Fig. 3A. Dashed lines indicate proposed thresholds for splitting and lumping lineages as species based on an empirical meta-analysis from Jackson et al. (2017).

exhibited several notable differences from the concatenated tree. First, unlike the concatenated tree (but similar to the BPP trees), the clade containing *G. infernalis\_NL, G. infernalis\_Gomas*, and *G. infernalis\_TX*, along with *G. mccoyi*, was not the sister taxon to *G. ophiurus*. Instead, it was recovered as the sister taxon to *G. infernalis\_DC* and *G. infernalis\_SHQG*. This relationship was close to strongly supported (PP = 0.93). Second, *G. infernalis\_Gomas* was weakly supported as the sister taxon to *G. infernalis\_NL* rather than to the clade with *G. infernalis\_TX* and *G. mccoyi*, which was also

weakly supported. Third, *G. liocephalus* was placed as the sister taxon to *G. infernalis* and *G. mccoyi*, with *G.* sp. Western as the sister taxon to these combined clades. However, these relationships were not strongly supported. Fourth, the monophyly of *G. ophiurus* was recovered but with weak support.

#### Hidden Diversity Assessment

The gdi estimates for the 12 evaluated lineages (Table 3) were calculated using the species tree topologies as guide

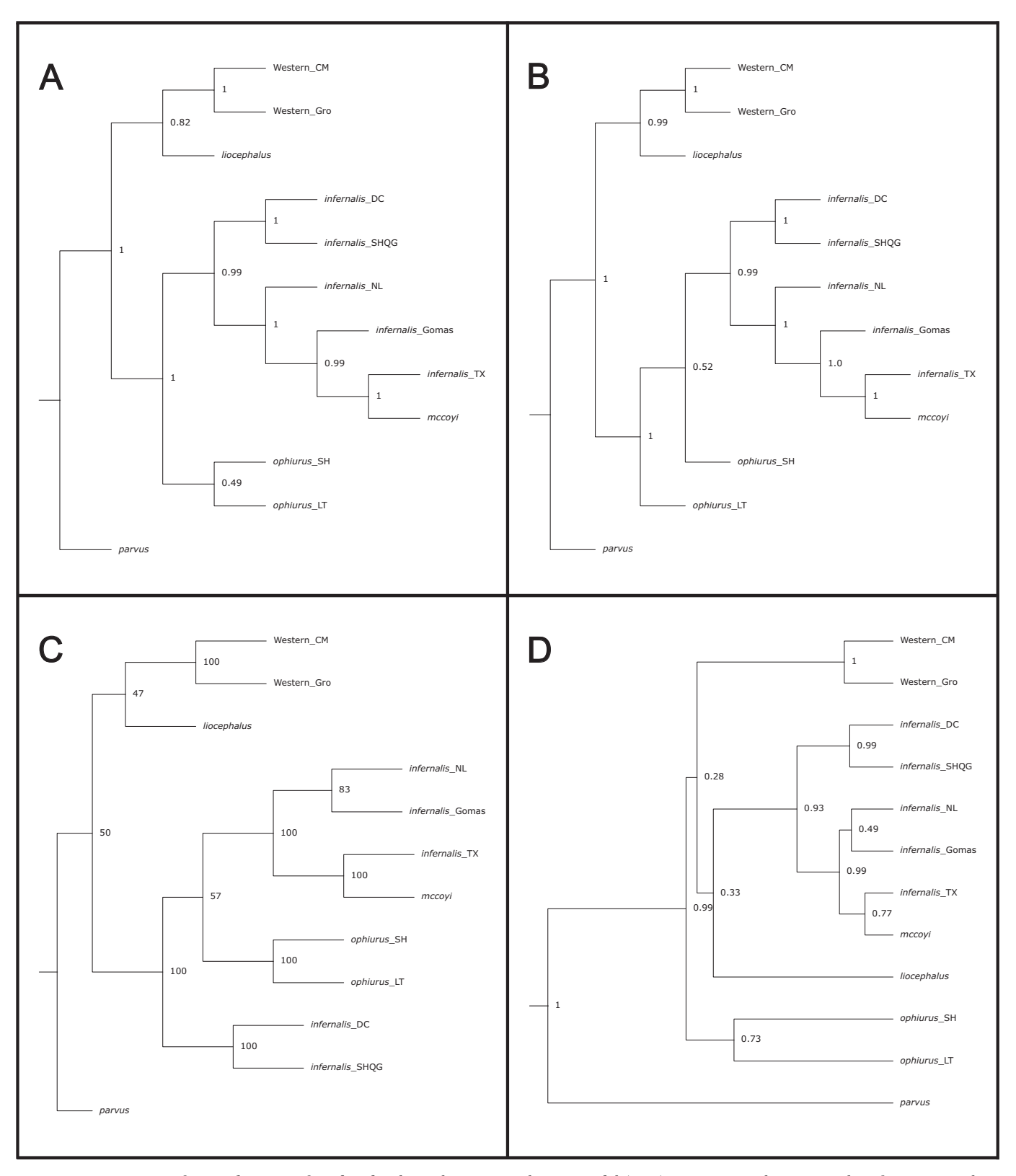


Fig. 3.—Species trees for *Gerrhonotus* inferred under the multispecies coalescent model (A, B). Best trees with support values from BPP analyses (each topology obtained in two out of four replicates). (C) Best tree with bootstrap support values from the SVDquartets analysis. (D) Species tree from the SNAPP analysis. Support values in (A), (B), and (D) are posterior probabilities.

trees in BPP. The assumed topology had little effect on the gdi estimates for these lineages. Nonetheless, some differences were observed. The gdi estimates for *G. infernalis\_*Gomas and *G. ophiurus\_*SH were slightly lower when using

the SVD quartets topology compared to estimates from other topologies. Conversely, estimates for *G. mccoyi* and *G. infernalis\_*TX were slightly and markedly higher, respectively, using the SVD quartets topology than those estimated using

Table 3.—Mean and range (in parentheses) of genealogical divergence index (gdi) estimates for the evaluated *Gerrhonotus* lineages across different species tree topologies. Species tree topologies correspond to those illustrated in Fig. 3. To interpret the gdi estimates, we followed the approach proposed by Leaché et al. (2019). This method employs thresholds derived from an empirical meta-analysis conducted by Jackson et al. (2017), which suggests that gdi values <0.2 suggest a single species, gdi values >0.7 suggest distinct species, and gdi values between 0.2 and 0.7 indicate ambiguous delimitation.

		g	di	
Lineage/topology	A (BPP)	B (BPP)	C (SVDquartets)	D (SNAPP)
G. infernalis_DC	0.78 (0.75-0.81)	0.78 (0.75-0.81)	0.79 (0.76-0.82)	0.78 (0.75–0.81)
G. infernalis_Gomas	0.65 (0.57-0.72)	0.65 (0.57-0.72)	0.59 (0.51-0.67)	0.67 (0.60-0.74)
G. infernalis_NL	0.31 (0.26-0.38)	0.31 (0.26-0.35)	0.30 (0.26-0.35)	0.28 (0.24-0.33)
G. infernalis_SHQG	0.43 (0.39-0.47)	0.42 (0.38-0.46)	0.43 (0.39-0.47)	0.42 (0.38-0.46)
G. infernalis_TX	0.49 (0.40-0.58)	0.49 (0.39-0.58)	0.66 (0.59-0.73)	0.49 (0.40-0.58)
G. liocephalus	0.88 (0.85-0.92)	0.88 (0.85-0.92)	0.89 (0.85-0.92)	0.88 (0.86-0.91)
G. mccoyi	0.87 (0.82-0.91)	0.87 (0.82-0.91)	0.92 (0.89-0.95)	0.87 (0.82-0.91)
G. ophiurus_SH	0.73 (0.69-0.76)	0.74 (0.71-0.77)	0.70 (0.66-0.74)	0.77 (0.73-0.80)
G. ophiurus_LT	0.98 (0.97-1.00)	0.98 (0.96-1.00)	0.98 (0.96-1.00)	0.99 (0.97-1.00)
G. parvus	0.99 (0.99-1.00)	0.99 (0.99-1.00)	1.00 (1.00-1.00)	1.00 (1.00-1.00)
G. sp. Western_CM	0.65 (0.61-0.69)	0.65 (0.60-0.70)	0.65 (0.61-0.70)	0.65 (0.61-0.69)
G. sp. Western_Gro	0.65 (0.60-0.70)	0.65 (0.60-0.70)	0.65 (0.60–0.70)	0.65 (0.60–0.69)

other topologies. Because of the minimal impact of the assumed topology on the gdi estimates, only the gdi estimates based on one of the BPP species tree topologies (Fig. 3A) are presented in Fig. 2.

Gerrhonotus parvus and G. liocephalus exhibited mean gdi estimates exceeding the distinct species threshold across all topologies (0.99–1.00 and 0.88–0.89, respectively). Among the potentially independent lineages, G. mccoyi and G. infernalis\_DC also displayed mean gdi estimates exceeding this threshold across all topologies (0.87-0.92 for G. mccoyi being distinct from the G. infernalis\_TX; 0.78-0.79 for G. infernalis\_DC being distinct from G. infernalis\_SHQG). Similarly, G. ophiurus\_LT and G. ophiurus\_SH displayed gdi estimates above the distinct species threshold across all topologies (0.98-0.99 for G. ophiurus\_LT being distinct from G. ophiurus\_SH; 0.70-0.77 for G. ophiurus\_SH being distinct from G. ophiurus\_LT). The two G. sp. Western lineages exhibited gdi estimates slightly below the distinct species threshold (0.65) across all tree topologies for being distinct from each other. Finally, gdi estimates for the remaining G. infernalis lineages fell within the ambiguous delimitation range, with values ranging from 0.28 (for G. infernalis\_NL being distinct from the G. infernalis\_Gomas) to 0.67 (for G. infernalis Gomas being distinct from G. infernalis\_NL).

#### DISCUSSION

## Phylogenetic Relationships of Gerrhonotus

Consistent with the molecular phylogeny of *Gerrhonotus* based on UCE data (Blair et al. 2022), our concatenated ML trees with the highest proportions of strongly supported nodes inferred a strongly supported clade composed of *Abronia* and *Barisia* as the sister taxon to *Gerrhonotus*. However, this sister-taxon relationship was not strongly supported (Fig. S2). On the other hand, as in that earlier study and another based on mitochondrial data (García-Vázquez et al. 2018a), we inferred from ddRADseq data here that *G. parvus* was the sister taxon to all remaining *Gerrhonotus* lineages in both the concatenated and species trees. These results underscore the robustness of this relationship across methodologies and datasets. However, some discordance was observed among the concatenated and species trees

inferred from ddRADseq data regarding the relationships among the remaining *Gerrhonotus* lineages.

As in previously published phylogenies of *Gerrhonotus* by García-Vázquez et al. (2018a) and Blair et al. (2022), the BPP species trees recovered a strongly supported clade containing all G. infernalis lineages, with G. mccoyi nested within it. The SNAPP species tree also recovered this G. infernalis-G. mccoyi clade, which had a high posterior probability (0.93). Therefore, it was unexpected that the concatenated tree showed the G. infernalis lineages forming two strongly supported, separate clades. Specifically, the clade composed of G. infernalis NL, G. infernalis Gomas, and G. infernalis TX, with G. mccoyi nested within it, was strongly supported as the sister taxon to G. ophiurus, rather than to the clade composed of G. infernalis\_DC and G. infernalis\_SHQG. The SVDquartets species tree retrieved both of these sister-taxa relationships. However, the relationship between the G. infernalis-G. mccoyi clade and G. ophiurus was weakly supported in the SVDquartets analysis.

The observed discordance between our concatenated and species trees may stem from limitations in the concatenated approach, as ML analysis on concatenated alignments is not statistically consistent under the multispecies coalescent model, and can be positively misleading (Mirarab et al. 2021). In contrast, the species tree estimation methods used in this study account for gene tree discordance due to incomplete lineage sorting, providing a statistically consistent approach under the multispecies coalescent model (Mirarab et al. 2021). Thus, despite the indication in our concatenated species tree of two separate clades of *G. infernalis*, the hypothesis of a single clade of *G. infernalis*, with *G. mccoyi* nested in it, appears to be the most plausible phylogenetic scenario for these taxa.

The following clades were generally well supported across both concatenated and species trees: (1) *G. infernalis\_NL*, *G. infernalis\_Gomas*, and *G. infernalis\_TX*, with *G. mccoyi* nested within it; (2) the sister-taxon relationship between *G. mccoyi* and the *G. infernalis\_TX*; and (3) the clade comprising *G. infernalis\_DC* and *G. infernalis\_SHQG*. However, the sister-taxon relationship between *G. mccoyi* and *G. infernalis\_TX* was not strongly supported in the SNAPP species tree (Fig. 3C). These three relationships were also

observed in the previous phylogeny by Blair et al. (2022), underscoring their consistency across analyses and data sets.

In contrast, the phylogenetic position of *G. infernalis*\_Gomas, which was not included in previous molecular studies, varied across analyses. Despite its geographic proximity to G. infernalis NL (Fig. 1), it was strongly supported as the sister taxon to the clade of *G. infernalis\_TX* and *G. mccoyi* in the concatenated and BPP species trees (Figs. 2 and 3A). Conversely, in the SVD quartets and SNAPP species trees, it was recovered as the sister taxon of G. infernalis\_NL, albeit with weak support in the SNAPP analysis. This phylogenetic incongruence highlights uncertainty in the placement of this lineage. Nonetheless, its strongly supported phylogenetic position in the concatenated and BPP species trees, combined with its geographic location in northwestern Nuevo León, suggest the possibility of historical admixture between the G. infernalis\_TX-G. mccoyi clade and G. infernalis\_NL. Further studies with denser sampling of populations are warranted to clarify these relationships.

Gerrhonotus ophiurus was strongly supported as monophyletic in both the concatenated (Fig. 2) and SVDquartets species trees (Fig. 3C). However, its monophyly was either weakly supported or not recovered in the BPP and SNAPP species trees. This discrepancy may stem from the representation of G. ophiurus\_LT by a single sample, which had data for only a limited percentage of loci (37.8%). This data limitation likely had a comparatively greater impact on support in analyses relying on fewer loci, such as those conducted for the BPP and SNAPP species trees. The mitochondrial phylogeny by García-Vázquez et al. (2018a) also recovered a strongly supported sister taxon relationship between G. ophiurus\_SH and G. ophiurus\_LT. However, in that phylogeny the G. ophiurus sample from Los Tuxtlas (also used in this study) formed a small, weakly supported clade with a sample from central Veracruz (Cuautlapan). In that study, the sister taxon to that clade was strongly supported and included populations from Hidalgo, San Luis Potosí, Querétaro, Tamaulipas, and another locality in central Veracruz (Misantla). This pattern suggests complex phylogenetic relationships within G. ophiurus, requiring additional sampling and analyses for full resolution. In the UCE phylogeny by Blair et al. (2022), G. ophiurus was strongly supported as monophyletic. However, that study did not include samples from the Los Tuxtlas region. Expanded sampling across the range of G. ophiurus, with a particular focus on the Los Tuxtlas region, is needed to clarify the taxonomic status of these G. ophiurus lineages further.

The G. sp. Western lineage was strongly supported as the sister taxon to G. liocephalus in our concatenated ML tree (Fig. 2). However, this relationship was strongly supported in only one of four BPP species tree replicates (with support values between 0.82 and 0.89 in the remaining replicates), and was weakly supported in the SVD quartets species tree. Meanwhile, the SNAPP species tree recovered the G. sp. Western lineage as the sister taxon to the G. infernalis—G. mccoyi clade and G. liocephalus, though with weak support. The phylogenetic placement of the G. sp. Western lineage has similarly varied across previous studies. In the mitochondrial tree by García-Vázquez et al. (2018a), the G. sp. Western lineage was weakly supported as the sister taxon to all other Gerrhonotus, except G. parvus and G. rhombifer. In the study by Blair et al. (2022), the G. sp. Western lineage

was strongly supported as the sister taxon to all other *Gerrhonotus* except *G. parvus* in their concatenated tree. In their SVDquartets species tree, however, the *G.* sp. Western lineage was weakly supported as the sister taxon to all *Gerrhonotus* excluding *G. parvus* and *G. liocephalus*. These inconsistencies highlight substantial uncertainty regarding the placement of the *G.* sp. Western lineage, reinforcing the need for further research to clarify its phylogenetic position. Nonetheless, we suggest that the morphological similarity between the *G.* sp. Western lineage and *G. liocephalus* (Good 1994), along with their geographic distributions following a recognized biogeographic pattern common in other taxa (e.g., McCranie et al. 2020), provides additional support for the sister-taxon relationship between these two taxa recovered in most of our analyses.

### Potential Hidden Diversity

Gerrhonotus mccoyi was recognized as a separate species based on its morphological distinctness, unique habitat, specialized ecology, and allopatric distribution in the Cuatro Ciénegas Basin, Coahuila (García-Vázquez et al. 2018b). High gdi estimates for G. mccoyi (0.87-0.92 across tree topologies for being distinct from G. infernalis\_TX) support its evolutionary independence and its recognition as a separate species from other Gerrhonotus taxa. However, although gdi estimates indicate that G. mccoyi is distinct from G. infernalis\_TX, they do not support the distinctness of G. infernalis\_TX from  $\dot{G}$ . mccoyi (gdi = 0.49-0.66 across tree topologies). This asymmetry likely reflects the sensitivity of gdi estimates to  $\theta$ , as lower genetic variability within a lineage often results in higher gdi values. This is particularly relevant for G. mccoyi, given its restricted distribution and presumably lower genetic diversity. Such dynamics can result in discordant gdi values for sister lineages with differing levels of intraspecific genetic variation (Barley et al. 2024). Interestingly, all phylogenetic analyses consistently placed G. mccoyi as more closely related to G. infernalis\_TX than to the geographically closer G. infernalis\_NL. This pattern of relationships suggests limited gene flow between G. mccoyi and G. infernalis\_NL despite their geographic proximity, further supporting the status of G. mccoyi as an independent evolutionary lineage. In addition, although it may be argued that recognizing G. mccoyi as a distinct species renders G. infernalis paraphyletic, it has been proposed that the monophyly requirement for species should be dropped, and that paraphyletic species or species consisting of multiple populations that are not monophyletic are common (Crisp and Chandler 1996; Kornai et al. 2024).

Like G. infernalis\_TX, the lineages G. infernalis\_Gomas and G. infernalis\_NL (the closest lineages to the clade G. infernalis\_TX lineage + G. mccoyi) also exhibited mean gdi estimates between 0.2 and 0.7 across all species tree topologies, indicating ambiguous species delimitation. However, gdi estimates consistently suggested that G. infernalis\_DC is a distinct species from the G. infernalis\_SHQG lineage (0.78–0.79). In contrast, gdi estimates for G. infernalis\_SHQG being distinct from G. infernalis\_DC ranged from 0.42 to 0.43, indicating ambiguous species delimitation. Given that six samples were analyzed for the G. infernalis\_DC lineage and three for the G. infernalis\_SHQG lineage, it is unlikely that these results are due to sampling

error. Again, this asymmetry may be due to the sensitivity of gdi estimates to  $\theta$ , which can result in discordant gdi values for sister lineages with differing levels of intraspecific genetic variation (Barley et al. 2024). These findings remain inconclusive and may be influenced by significant gaps in sampling. Further research is warranted to clarify the evolutionary independence of these lineages.

Good (1994:94) noted that the taxa austrinus, infernalis, liocephalus, loweryi, ophiurus, and taylori were historically "treated as conspecific because herpetologists are used to them being conspecific, and not because the evidence for or against conspecificity has been rigorously examined." He mentioned that G. taylori, described by Tihen (1954) from Clarines Mine, ca. 5 miles west of Santa Barbara, Chihuahua, was known from only two specimens, and considered the level of intraspecific variation to be insufficient to justify distinguishing G. taylori as a separate species, leading to its synonymization with G. infernalis. However, Lemos-Espinal and Smith (2007), among others, have since recognized G. taylori as a distinct species. Should G. infernalis\_DC prove to be evolutionary independent, the name G. taylori would be available for it.

The high gdi values for G. ophiurus\_SH and G. ophiurus\_LT across all tree topologies suggest that both may represent distinct species. This potential differentiation may be linked to the lack of known populations in the relatively large geographic gap between these sister lineages, which may have contributed to their divergence. Interestingly, Good (1994), in his taxonomic review of Gerrhonotus, assigned the only individual available to him from Los Tuxtlas to G. liocephalus rather than G. ophiurus. Alternatively, the high gdi values observed for both G. ophiurus lineages may be influenced by limited data coverage. Notably, the single sample of the G. ophiurus\_LT lineage had data for only a small percentage of loci (37.8%), which may have impacted the gdi estimates. Furthermore, our limited sampling of G. ophiurus likely fails to capture the full complexity of its phylogenetic relationships (see the foregoing), which could be more intricate than suggested by this preliminary assessment. The high gdi value observed for G. ophiurus\_LT may also reflect the sensitivity of gdi estimates to  $\theta$ , as lower genetic variability within a lineage typically results in higher gdi values. Given its restricted distribution in the Los Tuxtlas region, this lineage may harbor comparatively lower genetic diversity. To resolve the evolutionary relationships and clarify the taxonomic status of G. ophiurus lineages better, additional sampling across the full distribution of G. ophiurus, with particular emphasis on the Los Tuxtlas region, is necessary.

Our phylogenetic analyses corroborated the distinctness of the *Gerrhonotus* lineage distributed from Nayarit to Michoacán in western Mexico (our *G.* sp. Western\_CM lineage). This lineage was also documented as distinct in molecular studies with other types of data (García-Vázquez et al. 2018a; Blair et al. 2022). In addition, both our concatenated and species trees suggested that this lineage and the previously unknown *G.* sp. Western\_Gro lineage might represent two distinct evolutionary lineages. However, mean gdi values for these lineages being distinct from each other were identical (0.65) and indicated ambiguous species delimitation. Thus, the genetic differentiation between these lineages might reflect lack of sampling from regions between their populations (Fig. 1).

In summary, the boundaries between some of the potentially independent lineages identified in this study warrant further investigation. As noted in the foregoing, comprehensive sampling across large areas of Mexico is essential for advancing this research. Resolving these taxonomic uncertainties will help determine whether the observed divergences represent fully realized speciation events or merely the early stages of divergence leading to incipient species. Additionally, we used the genealogical divergence index (gdi) to conduct a preliminary assessment of the distinctness of the potentially independent lineages. This approach addresses concerns that lineages identified by BPP as distinct species sometimes correspond to populations rather than true species, raising issues of potential oversplitting by BPP (Leaché et al. 2019; Kornai et al. 2024). However, the gdi approach is not without its limitations. In addition to the concerns already noted (see the foregoing), the wide interval of uncertainty for gdi values (0.2 < gdi < 0.7) proposed by Jackson et al. (2017) has been criticized as indicative of the arbitrariness of this heuristic framework, and it has been suggested that the meta analysis underpinning these thresholds should be revisited using recent genomic data and improved analytical methods (Kornai et al. 2024). Such refinements could generate empirical estimates from well-studied systems where the species status of populations is well established, leading to more precise criteria and a narrower interval of uncertainly. Finally, some authors have stressed that genetic evidence for species delimitation should be complemented by other lines of evidence, including morphological and behavioral characteristics, as well as patterns of hybridization (e.g.,

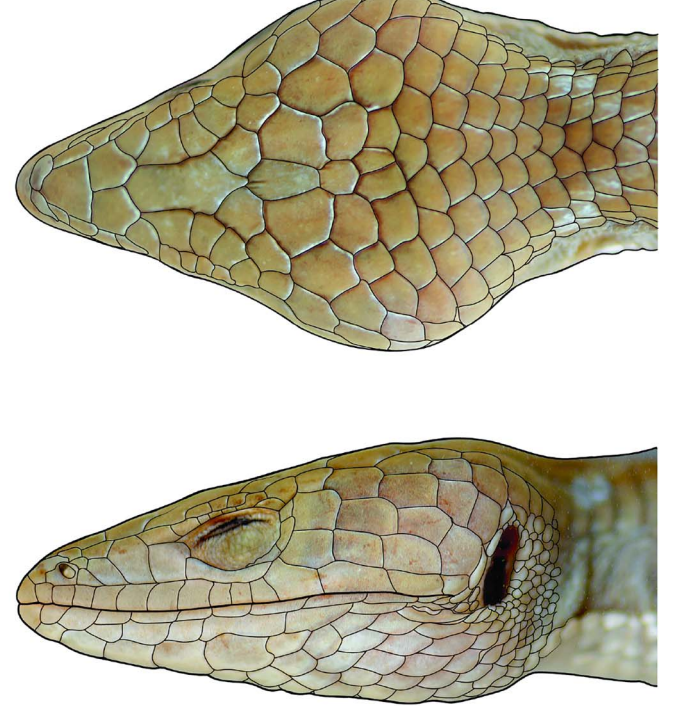
The gdi estimates for the two G. sp. Western lineages did not support them as distinct species. Furthermore, no obvious or consistent morphological differences were observed between specimens from these lineages by us, based on our examination of specimens listed in the following. Consequently, we tentatively assign the Guerrero populations to the same species as those from Colima and Michoacán, along with the populations from southern Nayarit, which were included in the study by García-Vázquez et al. (2018a) but not in ours. Good (1994) placed Gerrhonotus populations from southeastern Sinaloa and adjacent Durango in his isolated Sample 19. Although the geographic location of these populations suggests they may belong to G. sp. Western, a considerable geographic gap separates them from the populations assigned to this lineage in southern Nayarit. Therefore, we have chosen not to assign the populations from southeastern Sinaloa and adjacent Durango to G. sp. Western until genetic data become available. We formally describe the G. sp. Western lineage as a new species below.

Fujita et al. 2012; Solís-Lemus et al. 2015).

#### Species Description

Gerrhonotus **occidentalis** sp. nov. Gerrhonotus liocephalus: García and Ceballos 1994; Good 1994; Ramírez-Bautista 1994; Chávez-Ávila et al. 2015. [In part, misidentification.] (Figs. 4–7)

Holotype (Figs. 4, 5).—An adult male (MZFC-HE 8428, field number FSLG 1) from Jalisco, Sierra de Manantlán, Puerto Los Mazos (near the microwave tower), 19.6883333°N,



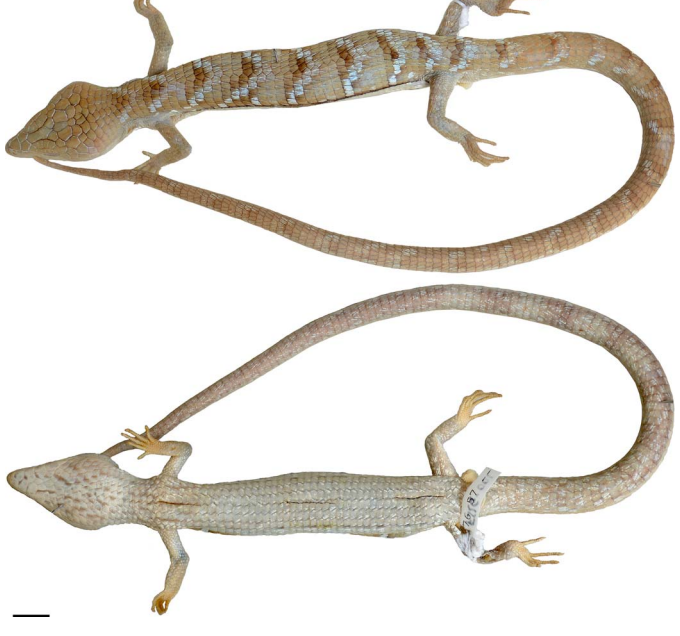


Fig. 5.—Gerrhonotus occidentalis. Dorsal (top) and ventral (bottom) views of holotype in preservative (MZFC-HE 8428; snout–vent length = 145.8 mm). Scale bar = 10 mm. A color version of this figure is available online.

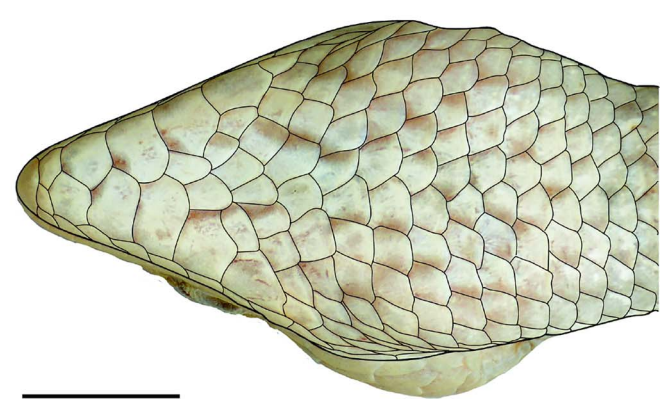


Fig. 4.—Gerrhonotus occidentalis. Dorsal (top), left lateral (middle), and ventral (bottom) views of the head of the holotype in preservative (MZFC-HE 8428; head length =  $30.9\,$  mm). Scale borders have been enhanced for easier discrimination. Scale bar =  $10\,$  mm. A color version of this figure is available online.

–104.3952778°W, 2500 m elevation, datum = WGS84 in all cases. Pine-oak forest. Collected by Javier López at approximately 1600 h on 6 December 1995.

Paratypes (Figs. 6, 7).—Eighteen; one from Jalisco: Chamela (MZFC-HE 32964); two from Michoacán: one from the Municipality of Chinicuila, near Puerto del Caimán, 18.67745°N, 103.40713°W, 1340 m (MZFC-HE 14110); and one from El Taguazal, approximately 25 km by road from Arteaga to Playa Azul, 18.23392°N, 102.24733°W, 757 m (MZFC-HE 32965). Nine from Colima: one from "Km 1.5 camino al Terrero," 19.42917°N, 103.94056°W, 1110 m (MZFC-HE 8038); one from approximately 1.4–2.4 km E La Central, 19.14900°N, 104.42647°W, 44 m (MZFC-HE 32963); three from the Municipality of Minatitlán, Mina Peña Colorada:

 $19.35978^{\circ}N,\ 104.07547^{\circ}W,\ 826$  m (MZFZ 4948-4949) and  $19.35853^{\circ}N,\ 104.07823^{\circ}W,\ 747$  m (MZFZ 5018); and four from the Municipality of Minatitlán, Cerro Moreno,  $19.35793^{\circ}N,\ 104.11960^{\circ}W,\ 938$  m (MZFZ 4950-4953). Six from Guerrero: three from the Municipality of Atoyac de Álvarez, La Florida,  $17.21944^{\circ}N,\ 100.36889^{\circ}W,\ 810$  m (MZFZ 4957-4959); and three from Puerto El Edén,  $17.46835^{\circ}N,\ 100.74510^{\circ}W$  (MZFZ 4954-4956).

Referred specimens.—COLIMA: vicinity of Colima (Museum of Vertebrate Zoology [MVZ] 197549; Good 1994); JALISCO: 40 miles north of Highway 80 on Highway 200 (CM 65825; Good 1994); 53 km NW (by Mexico Highway 200) of junction with Mexico Highway 80 (MVZ 205566; Good 1994); NAYARIT: Compostela, Mesillas (ISZ 665) (García Vázquez et al. 2018a). The ISZ number is a field number for a specimen pending cataloguing in the MZFC-HE.

**Diagnosis.**—This diagnosis is based on all specimens of the type series, excluding MZFZ 4956 (n = 18), and relevant literature (Good 1994; García-Vázquez et al. 2018b, and other sources cited therein).

Gerrhonotus occidentalis may be distinguished from G. farri, G. parvus, and G. rhombifer by having keeled dorsal scales (dorsal scales smooth in the latter species; García-Vázquez et al. 2018b), and from G. infernalis by having three scales in the canthal/loreal series (one canthal, one loreal, and one cantholoreal) and usually (in 94% of the specimens) prominent dark vertical bars on the lateral fold. In G. infernalis there are usually 4–5 scales in the canthal/loreal series (2 canthals and 2–3 loreals) and no dark vertical bars on the lateral fold (Good 1994; García-Vázquez et al. 2018b). Gerrhonotus occidentalis differs from G. mccoyi by usually having (in 94% of the specimens) prominent dark vertical bars on the lateral fold (dark vertical bars on the lateral fold usually absent in G. mccoyi; Good 1994; García-Vázquez et al.

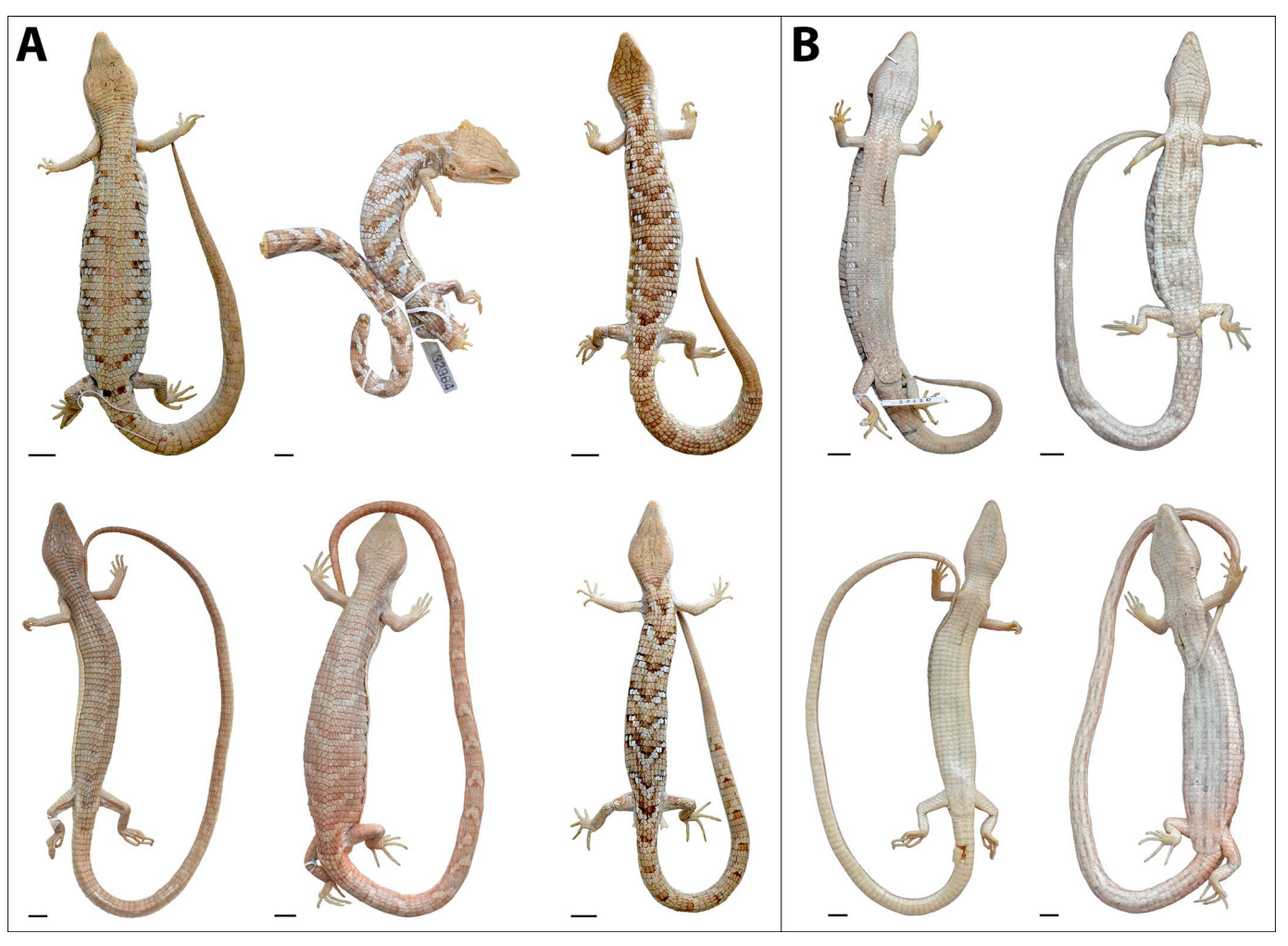


FIG. 6.—Variation in dorsal and ventral color pattern in adult specimens of *Gerrhonotus occidentalis* in preservative. (A) Variation in dorsal pattern. From left to right: top, MZFZ 4949, MZFC-HE 32964, and MZFZ 4953 (all from Colima); bottom, MZFZ 4955, MZFZ 4957, MZFZ 4959 (all from Guerrero). (B) Variation in ventral pattern. From left to right: top, MZFC-HE 14110, MZFZ 4951 (from Michoacán and Colima, respectively); bottom, MZFZ 4955, MZFZ 4957 (both from Guerrero). Scale bars = 10 mm.

2018b), and by lacking a dark mark extending from the temporal to the preocular or cantholoreal scales (present in G. mccoyi; García-Vázquez et al. 2018b). Gerrhonotus occidentalis may be distinguished from G. ophiurus by having one canthal, one loreal, and one cantholoreal in the canthal/ loreal series and a single preocular, whereas G. ophiurus usually has 2 canthals and  $\hat{2}$ –3 loreals and the preocular usually divided (in 92% and 75% of the specimens [n = 8], respectively; Good 1994). It also differs by lacking a dark mark extending from the temporal to the preocular or cantholoreal scales (present in G. ophiurus; García-Vázquez et al. 2018b). Gerrhonotus occidentalis differs from G. liocephalus by having (on average) more lamellae under the fourth toe (15–20, mean = 17.6, n = 18; vs. 12–17, mean = 14.3, n = 25 in G. liocephalus). Gerrhonotus occidentalis also has more combined supralabials than G. liocephalus  $(23-27, \text{ mean} = 24.8, n = 18; \text{ vs. } 22-26, \text{ mean} = 22.8, n = 18; \text{$ 25, in G. liocephalus specimens examined here; also, mean < 23, n = 110, in specimens of G. liocephalus examined by Good 1994). Finally, G, occidentalis also differs from G. liocephalus in lacking a dark, irregular line at the junction between the anteriormost temporals and supralabials (present in G. liocephalus).

**Description of holotype.**—Adult male; snout-vent length = 145.8 mm; head length = 30.9 mm; head width = 23.4 mm; tibia length = 14.7 mm; axilla-groin length = 79.3 mm; tail length = 295 mm.

Head scalation (Fig. 4).—Head scales flat, smooth. Snout rounded in dorsal and lateral views. Rostral nearly twice as wide as high (width = 3.32 mm; height = 1.8 mm), bordered posteriorly by one small medial postrostral and one slightly larger anterior internasal on each side of postrostral. Postrostral pentagonal, slightly wider than long, in broad contact laterally and posteriorly with anterior internasal and supranasal, respectively, on each side. Anterior internasals slightly wider than long, each in contact laterally with first supralabial and posteriorly with supranasal and nasal. Supranasals medially expanded, in medial contact with each other, approximately half as wide as long, obliquely oriented. Frontonasal large, roughly triangular, approximately as wide as long, in contact laterally with canthals on either side and posteriorly with prefrontals. Prefrontals slightly longer than wide; each in contact laterally with canthal, cantholoreal, and (narrowly) first superciliary, and posteriorly with frontal and first and (narrowly) second median supraoculars. Frontal

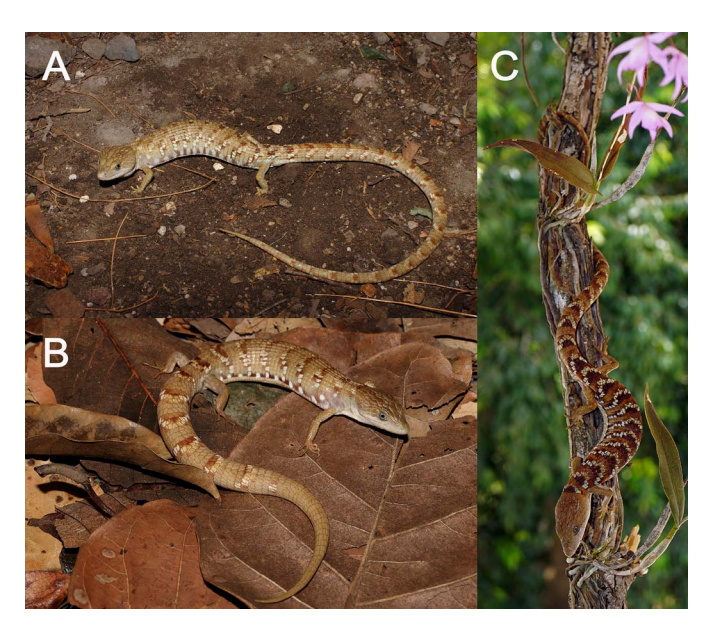


Fig. 7.—Gerrhonotus occidentalis in life. (A) Adult male (MZFZ 4951). (B) Adult female (MZFZ 4950). (C) Adult specimen from Colima, Cerro Alcomún. The latter photograph was taken by J. Jones on 29 December 2023. The specimen was released.

large, slightly more than twice as long as wide; in contact laterally with second and third median supraoculars and frontoparietal on either side, and (narrowly) posteriorly with interparietal. Frontoparietals approximately as wide as long, each in contact laterally with third and fourth median supraoculars, posterolaterally with upper primary temporal, posteriorly with parietal, and posteromedially with interparietal. Median supraoculars 5/5; second largest; first, third, and fourth subequal in size, approximately two-thirds as large as second, and slightly larger than fifth. Lateral supraoculars 4/3, much smaller than median supraoculars. Interparietal elongate; maximum length approximately twice maximum width; kite-shaped, enclosed narrowly by frontal, frontoparietals, parietals, and interoccipital; pineal eye undistinguishable. Parietals approximately as wide as long; nearly as long as interparietal, in contact anterolaterally with upper primary temporal, posterolaterally with a larger upper temporal (presumably representing fused upper secondary and upper tertiary temporals), posteriorly with occipital, and posteromedially with interoccipital. One row of postoccipitals, extending laterally to upper margin of ear on each side.

Canthus rostralis rounded, formed by two canthals followed posteriorly by one cantholoreal and first superciliary on left side; by one canthal followed posteriorly by one cantholoreal and first superciliary on right side. Canthals on left side small, slightly longer than wide; single canthal on right side elongate, nearly thrice as long as wide. Nasal slightly elongate antero-posteriorly, with naris situated posteriorly; separated from rostral by first supralabial and anterior internasal. Postnasals 2/2, small, subequal in size; followed posteriorly by one loreal, one cantholoreal, and one preocular scales on each side of snout. Loreal nearly as high as combined postnasals, slightly narrower than cantholoreal and preocular. Cantholoreal approximately as high as canthal and loreal combined, in contact anteriorly with canthal and loreal, medially with prefrontal, posteriorly with first superciliary and preocular, and ventrally with fifth supralabial on left side and fourth (narrowly) and fifth supralabials on right side. Preocular slightly higher than wide; approximately as wide as cantholoreal. Suboculars 1/1, longitudinally elongate, extending to level of posterior end of orbit; postoculars 3/3. Superciliaries 7/6; first superciliary largest; followed posteriorly by gradually shallower superciliaries except last superciliary much higher than penultimate one. Supralabials 13/13; posterior-most three larger and higher than anterior ones. Temporal scales in five rows. Primary temporals 4/4, lower primary temporal in contact with 11th and 12th supralabials on either side. Upper secondary and upper tertiary temporals presumably fused into one large scale in dorsal contact with parietal and occipital on either side; 3/3 and 4/4 secondary and tertiary temporals, respectively, extending ventrally from presumably fused upper secondary and upper tertiary temporal scales. Lower secondary and lower tertiary temporals in contact with 12th and 12th (narrowly) and 13th supralabials on left side; with 12th supralabial and 13th supralabial and following scale posteriorly on right side.

Mental nearly twice as wide as long. Infralabials 10/11; first two as deep as, or slightly deeper than, adjacent supralabials; much deeper than remaining infralabials. Sublabials 6/7; anterior-most in contact with second infralabial; all deeper than adjacent infralabials. Two postmentals. Chinshields 5/5; those of first two pairs in broad contact with each other, fifth one on left side much smaller than anterior ones and about as large as adjacent medial scales. External ear opening oval, vertically elongate (maximum width and maximum height 2.5 mm and 5.2 mm and 2.3 mm and 5.0 mm on left and right sides, respectively), without lobules or spines.

**Body scalation.**—Dorsal scales keeled, imbricate, nearly equal in size to ventrals; in 10 longitudinal rows on neck, and in 14 rows of full-sized scales and 1 row of reduced lateral dorsals (approximately half as large as full-sized dorsals in average) at level of midbody; in 48 transverse rows from first row of nuchals to last scale row lying at least partially over posterior portion of thighs. Lateral fold well developed. Ventral scales in 46 transverse rows from level of anterior insertion of forelimbs to vent; in 12 longitudinal rows at level of midbody. Precloacal scales 6; medial largest, gradually smaller laterally; medial pair nearly twice as large as lateral ones. Scales on forelimbs generally large, smooth, imbricate except smaller, barely or not imbricate on ventral surface of arms; scales on posterior limbs similarly large, smooth, imbricate, except much smaller, not imbricate on posterior surface of thighs. Supradigital scales in one row. Subdigital lamellae on manus I 5/5, II 9/9, III 14/13, IV 13/14, V 9/9. Subdigital lamellae on pes I 5/6, II 10/10, III 14/14, IV 17/18, V 13/12. Tail whorls 130. Hemipenes partially everted.

Color pattern (in preservative; Fig. 5). Body dorsal surface with olive-gray (42) background color and nine dark-edged, white crossbands (white crossbands hereafter for simplicity): one on neck, one between levels of anterior and posterior insertions of arms, and seven between levels of axilla and vent. On flanks, white crossbands consisting of two short series, one dorsal scale in width each, of dark-edged white scales extending along adjacent transverse scale rows but typically across different or partly different longitudinal scale rows, occasionally flanked laterally by scattered dark scales; on middorsum, white crossbands V-shaped, 1–2 dorsal scales in width (some scales with only white keels), flanked

anteriorly by distinctly darker scales. Tail with similar darkedged, white crossbands; distinct on anterior end; gradually becoming less distinct posteriorly. Lateral fold with 11/12 dark bars alternating with light bars, each dark bar roughly two dorsal scales wide.

Body ventral surface background color pinkish buff (121D); numerous drab-gray (199D), irregular spots scattered on throat; venter with narrow dark stripe on medial half of third scale row flanked laterally by white stripe on upper half of third scale row and lower half of second scale row on each side; dark and white stripes mostly fragmented, composed of 9/9 short scale series (1–4 scales long) bearing prominent dark and white spots, respectively, separated from each other by mostly unmarked scales; chest and abdomen between third scale rows covered with diffuse, gray (glaucus 80) pigment except for few white scattered specks. Ventral surface of hind limbs and tail covered with drabgray (199D) pigment except for some ill-defined, white-cream bands on anterior half of tail and abundant, small, irregular white marks on limbs and tail.

**Variation.**—This section is based on all specimens of the type series, excluding MZFZ 4956 (n = 18, unless otherwise noted). The examined specimens comprise eight males, two females, and eight of unknown sex. One canthal, one loreal, one cantholoreal, and one preocular on each side in all specimens with the following exceptions: canthal fused with internasal on one side in two specimens, on both sides in one; two canthals on one side in one specimen. Cantholoreal split horizontally into two scales on one side in two specimens, on both sides in three. One small scale at junction of loreal, cantholoreal, preocular, and supralabial scales on both sides in one specimen; one small triangular scale at junction of loreal, cantholoreal, and supraocular scales on one side in one specimen. Combined supralabials 23-27 (mean = 24.8; n = 18). Transverse dorsal scale rows 47-53(mean = 49.8; n = 18). Longitudinal dorsal scale rows 16, with no reduced scales flanking them (lateral dorsal scales as large as any dorsal), in four specimens; 14 rows of full-sized scales with reduced lateral dorsals in remaining specimens: latter scales from approximately half to slightly more than half the size of other dorsals in five specimens, less than half the size of other dorsals in eight specimens, and slightly more than half the size of other dorsals on one side, and less than half that size on other side in one specimen. Caudal whorls in specimens with complete tail 129–145 (mean = 136.7, n = 6). Subdigital scales on fourth to 15–20 (mean = 17.6, n = 18).

**Color pattern (in preservative).**—In the following description of variation in color pattern we included the holotype, but not a road-killed specimen (MZFC-HE 32965). Thus, the description is based on the remaining 17 specimens.

**Dorsal pattern (Fig. 6).**—Body dorsal general pattern consisting of drab (27) to smoke gray (45) background color with usually one or two white crossbands anterior to level of axilla and 6–9 between levels of axilla and groin visible on flanks, but often faint or indiscernible on middorsum. Variation in this general pattern included the following: background color drab (27) in three specimens; light drab (199C) in four; drab-gray (119D) in five; olive gray (42) in one; smoke gray (44–45) in four. One white crossband above level of anterior insertion of arms and none, one, and two

crossbands on neck in three, nine, and one specimen, respectively; one and two crossbands on neck in one specimen each; no white crossbands anterior to level of axilla in remaining two specimens.

White crossbands on flanks between levels of axilla and groin 6–9 (6/6, 7/7, 8/8, and 9/9 in two, six, two, and one specimen, respectively; 6/7 in one; 8/7 in one; and 9/8 in four), consisting of 1–3 short series, one dorsal scale in width each, of dark-edged white scales extending along adjacent transverse rows but typically across entirely or only partly different longitudinal scale rows, rarely flanked laterally by scattered dark scales. White crossbands extending across middorsum along entire length of body in 10 specimens (weakly to barely distinguishable in six); only 1–2 extending across middorsum on posterior fourth of body in five (faint in all); undistinguishable on middorsum in remaining two specimens. White crossbands extending across middorsum V-shaped, 1–2 dorsal scales in width, generally less evident than on flanks; from lacking any dark flanking scales to flanked by few, scattered dark scales to flanked by full dark crossbands. Lateral fold with 11-13 dark bars (indistinct to conspicuous, 1-2 dorsal scales in width) alternating with white bands in all specimens, except barely distinguishable

Ventral pattern (Fig. 6).—Ventral surface background color usually (in 14 specimens) white to white-cream; pale horn (92) in one specimen; pale pinkish buff (121D) in two. Throat with few pearl gray (81) or drab-gray (119D) longitudinal streaks (especially on sides) in 11 and one specimen, respectively; with numerous drab-gray (199D) spots in one specimen; immaculate in remaining four specimens. Body ventral surface with one narrow dark stripe on medial half of third scale row flanked laterally by one wider white stripe on upper half of third scale row, second scale row, and first scale row (in part) in three specimens; dark and white stripes seemingly fragmented, composed of 7–11 short scale series (1–4 scales long) bearing prominent dark and white spots, respectively, separated from each other by scales bearing much fainter dark and white spots or unmarked scales in 13 specimens; dark and white stripes absent in remaining specimen. Rest of venter with abundant small, faint, diffuse glaucus (80) spots (often covering most of chest and especially belly scales) in 16 specimens (spots forming one midventral narrow stripe in six; some scattered white specks in four); venter immaculate except for pearl gray (81) scale margins in remaining specimen.

Color pattern in life (Fig. 7).—Photographs of two of the examined specimens (MZFZ 34950, adult female, and MZFZ 4951, adult male) in life, along with a photograph of a specimen in his habitat (not examined) are shown in Fig. 7. All of these specimens are from Colima. A photograph of a specimen in life from Chamela, Jalisco, is shown in Castiglia et al. (2010:Fig. 2). No photographs of living specimens from Guerrero were available.

**Sexual dimorphism.**—Distinguishing the sexes in *Gerrhonotus* specimens can be challenging because of the lack of pronounced sexual dimorphism, and a detailed investigation of this topic is beyond the scope of this study. However, in five adult males from Colima and Jalisco (SVL = 140-146 mm), the head width–to–head length (HW/HL) ratio ranged from 0.70 to 0.78 (mean = 0.74), which was slightly higher than that observed in two adult females from Colima

and Michoacán (SVL = 138.7–158.0 mm; HW/HL ratio = 0.70–0.71, mean = 0.69). Notably, two males from Mina Peña Colorada, Colima (AEVB120 and AEVB122), exhibited slightly wider heads than a female of similar size from the same locality (males, SVL = 140.2–143.4 mm, HW/HL ratio = 0.74–0.78; female, SVL = 139.7 mm, HW/HL ratio = 0.70).

García-Bastida et al. (2013) previously documented that males of G. infernalis possess larger heads and bodies than females. Our limited data similarly suggest that males of G. occidentalis may have relatively larger heads than females. However, among the sexed specimens, the largest individual was a female (SVL = 168 mm), exceeding the size of all adult males (see above), and the largest specimen in our entire sample was presumably a female (SVL = 166 mm, HW/HL ratio = 0.62).

Among the five specimens of G. occidentalis from Guerrero, the four largest individuals (SVL = 135.8-166.0 mm) lacked everted hemipenes, and their HW/HL ratios (0.62-0.68, mean = 0.64) suggest they may be females. If this is accurate, their head proportions might reflect geographic variation rather than solely sexual dimorphism.

Etymology.—The name *occidentalis* derives directly from the Latin word "occidentalis," meaning of the west, pertaining to, or characteristic of the western regions of the earth (Brown 1956). This refers to the geographic distribution of the new species in western Mexico. This species has been previously referred to as "G. 'western" (García-Vázquez et al. 2018a), "G. cf. *liocephalus* from western Mexico" (García-Vázquez et al. 2018b), and "G. sp. 'western" (Blair et al. 2022).

**Distribution and ecology.**—We were not able to include in this study a specimen from "Nayarit: Compostela: Mesillas" (ISZ-665). This specimen was included by García-Vázquez et al. (2018a) in their mitochondrial phylogeny of Gerrhonotus. In that phylogeny, the specimen formed a clade with other specimens from Colima (ANMO1097 = MZFC-HE 32965) and Michoacán (ANMO 1167 = MZFC-HE 32963) included in the UCE phylogeny (Blair et al. 2022) and with another specimen from Michoacán included here (ANMO 526 = MZFC-HE 14110). Thus, G. occidentals is known to occur on the Pacific slopes of Mexico from southern Nayarit through Jalisco, Colima, and Michoacán to central Guerrero. It is worth noting that Woolrich-Piña et al. (2016) reported G. liocephalus from the Sierra Madre Occidental and Trans-Mexican Volcanic Belt physiographic regions of Nayarit and from the Sierra de Vallejo-Río Ameca and Sierra de San Juan Natural Protected Areas in Nayarit. Whether these records truly represent G. liocephalus or instead G. occidentalis is unknown. The geographically closest congener of G. occidentalis is G. liocephalus, as the distributions of these two species generally appear to extend on the opposite versants of the Sierra Madre Occidental, Trans-Mexican Volcanic Belt, and Sierra Madre del Sur. However, they do approach each other in some places. The records of G. liocephalus from Las Fundiciones and of G. occidentalis from Puerto El Edén and Atoyac de Álvarez are both on the Pacific Versant of central Guerrero and are only ~50 km (airline) or less from each other, suggesting that these species are parapatric or even sympatric in parts of their geographic distributions.

Gerrhonotus occidentalis is poorly known from Nayarit, Michoacán, and Guerrero, but has been reported from the Chamela-Cuixmala Biosphere Reserve region on the coast of Jalisco (as G. liocephalus) since the early 1990s (García and Ceballos 1994; Ramírez-Bautista 1994). The species is even featured on the cover of one of those reports (Ramírez-Bautista 1994). In this region, G. occidentalis is reported to inhabit tropical deciduous forest (or dry forest), tropical semideciduous forest, and riparian vegetation, where it may be found in leaf litter on the forest floor, on bushes, and under rocks, and is regarded as a terrestrial, arboreal, and (may be inaccurately) "fossorial" species (García and Ceballos 1994). Outside this region, G. occidentalis also is known to occur in oak forest (the two paratypes from Michoacán) and pine-oak forest (the holotype). One of the paratypes (MZFC-HE 32963) was collected near the town of La Central, Colima, in an area with mango and lemon crops. The specimens from Guerrero were found near agricultural areas, perched on bushes or rock walls. Overall, G. occidentalis is known to occur from nearly sea level (44 m) to about 1500 m of elevation. García and Ceballos (1994), Ramírez Bautista et al. (1994), and García and Cabrera-Reves (2008) provided lists of other amphibians and reptiles in the Chamela region, and the latter also evaluated the effect of the environmental seasonality and vegetation structure on the spatial and temporal patterns of the amphibian and reptile community in the region, although they did not include Gerrhonotus occidentalis (as G. liocephalus) in their list. Finally, with regard to its diet and reproduction, G. occidentalis is a carnivorous and oviparous species (García and Ceballos 1994). Field observations of populations in Colima indicate that mating occurs from December to February, with females laying 6–29 eggs between February and April. Eggs hatch approximately 40–45 d later. Also, fecal analysis of a collected specimen revealed remains of orthopterans, coleopterans, and hemipterans (J. Jones, personal communication).

**Remarks.**—*Gerrhonotus occidentalis* is known by the common names of "alicante" in the Chamela-Cuixmala Biosphere Reserve region on the coast of Jalisco, and "escorpión" in Guerrero and Michoacán.

The collecting localities for two specimens of *Gerrhonotus* sp. Western included in this study (FJLG 001 or MZFC-HE 8428 and MZFC-HE 32965) are given in error as "Chamela" in García Vázquez et al. (2018a,b) and "Michoacán, Chinicuila, close to Puerto el Caimán" in García-Vázquez et al. (2018b), respectively.

The karyotype of a specimen of G. occidentalis from Chamela, Jalisco, showed 2n=38 chromosomes, and it was composed of 14 macrochromosomes and 24 microchromosomes. All the macrochromosomes seemed biarmed but some doubt existed about the morphology of the smallest ones (Castiglia et al. 2010).

Cope (1896) stated that the hemipenis is bifurcate in *Barisia* and *Gerrhonotus*, and García-Vázquez et al. (2018a) similarly reported distal bifurcation of the hemipenis in *G. mccoyi*. The hemipenis morphology of *G. occidentalis* was previously unknown. Through examination of the eight males with everted hemipenes in our sample, we documented that these organs are also distally bifurcate in this species. However, full eversion was observed in only four individuals. These included three juveniles and one adult male. In the adult specimen (MZFZ 4948, SLV = 143.4 mm), the left hemipenis measured 7.7 mm in length, with each distal "horn" approximately 2.4 mm long, whereas the right hemipenis measured 9.5 mm in length, with distal horns

approximately 3.3 mm long. The proximal half of the truncus was smooth, whereas its distal half and the distal horns were covered with transverse rows of small calyces. The distal horns were evident in all males with fully everted hemipenes and two specimens with partially everted hemipenes. In all males with partially or fully everted hemipenes, the surface was calyculate.

Conservation.—Castiglia et al. (2010) and Chávez-Ávila et al. (2015) reported G. liocephalus as classified in the "Sujeta a protección especial" (subject to special protection) category on the Norma Oficial Mexicana 059 (NOM-059) list (SEMARNAT 2010) and the "Least concern" category of the International Union for Conservation of Nature Red List of Threatened Species (Vázquez-Díaz and Quintero-Díaz 2007), respectively. These works focused on the herpetofauna from the Chamela region and the state of Jalisco, respectively. Therefore, they dealt with populations of G. occidentalis on the Pacific slopes of Jalisco. However, in the above classifications, the authors treated those populations as G. liocephalus, even though Castiglia et al. (2010) raised serious doubts about their taxonomic status (see the foregoing), suggesting that these classifications are likely not suitable for G. occidentalis. Thus, G. occidentalis is yet to be included in the aforementioned classifications.

Gerrhonotus occidentalis is considered venomous by the local population in the Chamela region, where the species was considered as "poco abundante" (rare) by García and Ceballos (1994). Using the assessment framework provided by Wilson et al. (2013), we evaluated the environmental vulnerability score or EVS (another scheme for ranking the imperilment of amphibians and reptiles revised for Mexico) for G. occidentalis as follows. We considered that (1) its geographic distribution is only within Mexico, but its distribution is not restricted to the vicinity of the type locality; (2) it occurs in at least four vegetation formations (tropical deciduous forest, tropical semideciduous forest, oak forest, and pine-oak forest); and (3) it is a terrestrial and/or arboreal species thought to be harmful and might be killed on sight. Therefore it has an EVS of 5 + 5 + 4 = 14 out of 20. This score puts it in the category of high vulnerability.

Acknowledgments.—Support for this work was provided by the Dirección General de Apoyo al Personal Académico, Universidad Nacional Autónoma de México (PAPIIT grant numbers IN218522 to ANMO and IN-218022 to UOGV), and the Consejo Nacional de Ciencia y Tecnología (CONACyT A1-S-37838) to UOGV. We thank R. Cervantes-Burgos, A. Vité-Hernández, R. G. Escobedo-Cadena, A. García-Vinalay, R. G. Martínez-Fuentes, P. Ponce-Campos, D. Lazcano, U. García-Sotelo, A. E. Valdenegro-Brito, and especially W. Schmidt-Ballardo, the late F. Mendoza-Quijano, and J. Jones for assistance with fieldwork and donation of samples; D. Lara-Tufiño, D. I Sánchez-Aguilar, A. E. Valdenegro-Brito, and S. Lambert for assistance with lab work; A. E. Valdenegro-Brito and J. Jones for help with photographs; M. Monroy-Sánchez, D. Lara-Tufiño, and H. Archundia-Nieto for assistance with figures. Comments from two anonymous reviewers greatly improved the manuscript. We also thank Adam Leaché for his valuable advice, and G. Campillo-García for cataloguing specimens at the MZFC. ANMO thanks the Programa de Apoyos para la Superación del Personal Académico (PASPA), Universidad Nacional Autónoma de México, for financial support during a sabbatical stay at the Museo Nacional de Ciencias Naturales in Madrid in the fall of 2023, and I. de la Riva for hosting him during this period and helping with analyses. All specimens were collected under permits issued to ANMO (permit FAUT-0093) and UOGV (permit FAUT-0246) by the Secretaría de Medio Ambiente y Recursos Naturales of the Mexican government.

#### SUPPLEMENTAL MATERIAL

Supplemental material associated with this article can be found online at https://doi.org/10.1655/Herpetologica-D-24-00004.S1 and https://doi.org/10.1655/Herpetologica-D-24-00004.S2.

#### LITERATURE CITED

- Andrews, S. 2010. FastQC: A quality control tool for high throughput sequence data. Available at http://www.bioinformatics.babraham.ac.uk/projects/fastqc. Accessed on 15 October 2023. Babraham Institute, UK.
- Banda-Leal, J., M. Nevárez-de los Reyes, and R.W. Bryson, Jr. 2017. A new species of Pygmy Alligator Lizard (Squamata: Anguidae) from Nuevo León, México. Journal of Herpetology 51:223–226.
- Barley, A.J., A. Nieto-Montes de Oca, N.L. Manríquez-Morán, and R.C. Thomson. 2024. Understanding species boundaries that arise from complex histories: Gene flow across the speciation continuum in the Spotted Whiptail Lizards. Systematic Biology 73:901–919.
- Blair, C., R.W. Bryson, Jr., U.O. García-Vázquez, A. Nieto-Montes de Oca, D. Lazcano, J.E. McCormack, and J. Klicka. 2022. Phylogenomics of alligator lizards elucidate diversification patterns across the Mexican transition zone and support the recognition of a new genus. Biological Journal of the Linnean Society 135:25–39.
- Bouckaert, R., T.G. Vaughan, J. Barido-Sottani, ... A.J. Drummond. 2019. BEAST 2.5: An advanced software platform for Bayesian evolutionary analysis. PLOS Computational Biology 15:e1006650.
- Brown, R.W. 1956. Composition of Scientific Words. Smithsonian Institution Press, USA.
- Bryson, R.W., Jr., and M.R. Graham. 2010. A new alligator lizard from northeastern Mexico. Herpetologica 66:92–98.
- Castiglia, R., F. Annesi, A.M.R. Bezerra, A. García, and O. Flores-Villela. 2010. Cytotaxonomy and DNA taxonomy of lizards (Squamata, Sauria) from a tropical dry forest in the Chamela-Cuixmala Biosphere Reserve on the coast of Jalisco, Mexico. Zootaxa 2508:1–29.
- Chávez-Ávila, S.M., G. Casas-Andreu, A. García-Aguayo, J.L. Cifuentes-Lemus, and F.G. Cupul-Magaña. 2015. Anfibios y Reptiles del Estado de Jalisco. Análisis Espacial, Distribución y Conservación. Universidad de Guadalajara, México.
- Chifman, J., and L. Kubatko. 2014. Quartet inference from SNP data under the coalescent model. Bioinformatics 30:3317–3324.
- Clause, A.G., R. Luna-Reyes, and A. Nieto-Montes de Oca. 2020. A new species of Abronia (Squamata: Anguidae) from a protected area in Chiapas, Mexico. Herpetologica 76:330–343.
- Conroy, C.J., R.W. Bryson, Jr., D. Lazcano, and A. Knight. 2005. Phylogenetic placement of the Pygmy Alligator Lizard based on mitochondrial DNA. Journal of Herpetology 39:142–147.
- Cope, E.D. 1896. On the hemipenes of the Sauria. Proceedings of the Academy of Natural Sciences of Philadelphia 48:461–467.
- Crisp, M.D., and G.T. Chandler. 1996. Paraphyletic species. Telopea 6:813–
- Eaton, D.A.R., and I. Overcast. 2020. ipyrad: Interactive assembly and analysis of RADseq datasets. Bioinformatics 36:2592–2594.
- Edgar, R.C. 2004. MUSCLE: A multiple sequence alignment method with reduced time and space complexity. Nucleic Acids Research 32:1792– 1797.
- Flouri, T., X. Jiao, B. Rannala, and Z. Yang. 2018. Species tree inference with BPP using genomic sequences and the multispecies coalescent. Molecular Biology and Evolution 35:2585–2593.
- Fujita, M.K., A.D. Leaché, F.T. Burbrink, J.A. McGuire, and C. Moritz. 2012. Coalescent-based species delimitation in an integrative taxonomy. Trends in Ecology & Evolution 27:480–488.
- García, A., and A. Čabrera-Reyes. 2008. Estacionalidad y estructura de la vegetación en la comunidad de anfibios y reptiles de Chamela, Jalisco, México. Acta Zoológica Mexicana (nueva serie) 24:91–115.
- García, A., and G. Ceballos. 1994. Guía de Campo de los Reptiles y Anfibios de la Costa de Jalisco, México/Field Guide to the Reptiles and Amphibians of the Coast of Jalisco, Mexico. Fundación Ecológica of Cuixmala, A.C. Instituto de Biología, U.N.A.M. Fundación Ecológica de Cuixmala, Mexico.
- García-Bastida, M., D. Lazcano, L.D. McBrayer, and R. Mercado-Hernández. 2013. Sexual dimorphism in the alligator lizard Gerrhonotus infernalis (Sauria: Anguidae): Implications for sexual selection. The Southwestern Naturalist 58:202–208.

Downloaded from http://meridian.allenpress.com/herpetologica/article-pdf/doi/10.1655/Herpetologica-D-24-00004/3533869/10.1655\_herpetologica-d-24-00004.pdf by Mexico, Uri Garcia on 05 August 2025

- García-Vázquez, U.O., A. Nieto-Montes de Oca, R.W. Bryson, W. Schmidt-Ballardo, and C.J. Pavón-Vázquez. 2018a. Molecular systematics and historical biogeography of the genus Gerrhonotus. Journal of Biogeography 45:1640–1652.
- García-Vázquez, U.O., A. Contreras-Arquieta, M. Trujano-Ortega, and A. Nieto-Montes de Oca. 2018b. A new species of Gerrhonotus (Squamata: Anguidae) from the Cuatro Ciénegas Basin, Coahuila, Mexico. Herpetologica 74:269–278.
- Good, D.A. 1994. Species limits in the genus *Gerrhonotus* (Squamata: Anguidae). Herpetological Monographs 8:180–202.
- Jackson, N.D., B.C. Carstens, A.E. Morales, and B.C. O'Meara. 2017. Species delimitation with gene flow. Systematic Biology 66:799–812.
- Knight, R.A., and J.F. Scudday. 1985. A new Gerrhonotus (Lacertilia: Anguidae) from the Sierra Madre Oriental, Nuevo León, Mexico. The Southwestern Naturalist 30:89–94.
- Kornai, D., X. Jiao, J. Ji, T. Flouri, and Z. Yang. 2024. Hierarchical heuristic species delimitation under the multispecies coalescent model with migration. Systematic Biology 73:1015–1037.
- Leaché, Á.D., B.L. Banbury, J. Felsestein, A. Nieto-Montes de Oca, and A. Stamatakis. 2015. Short tree, long tree, right tree, wrong tree: New acquisition bias corrections for inferring SNP phylogenies. Systematic Biology 64:1032–1047.
- Leaché, A.D., T. Zhu, B. Rannala, and Z. Yang. 2019. The spectre of too many species. Systematic Biology 68:168–181.
- Lemos-Espinal, J.Á., and H.M. Smith. 2007. Anfibios y Reptiles del Estado de Coahuila, México/Amphibians and Reptiles of the State of Coahuila, Mexico. CONABIO, Mexico.
- McCartney-Melstad, E., M. Gidis, and H.B. Shaffer. 2019. An empirical pipeline for choosing the optimal clustering threshold in RADseq studies. Molecular Ecology Resources 19:1195–1204.
- McCranie, J.R., S. Matthews, and B. Hedges. 2020. A morphological and molecular revision of lizards of the genus *Marisora* Hedges & Conn (Squamata: Mabuyidae) from Central America and Mexico, with descriptions of four new species. Zootaxa 4763:301–353.
- Mirarab, S., L. Nakhleh, and T. Warnow. 2021. Multispecies coalescent: Theory and applications in phylogenetics. Annual Review of Ecology, Evolution, and Systematics 52:247–268.
- Peters, W.C.H. 1876. Über neue Arten der Sauriergattung Gerrhonotus. Monatsberichte der Königlichen Preussische Akademie des Wissenschaften zu Berlin 1876:297–330.
- Peterson, B.K., J.N. Weber, E.H. Kay, H.S. Fisher, and H.E. Hoekstra. 2012. Double digest RADseq: An inexpensive method for de novo SNP discovery and genotyping in model and non-model species. PLoS One 7:1–11.
- Pyron, R.A., F.T. Burbrink, and J.J. Wiens. 2013. A phylogeny and revised classification of Squamata, including 4161 species of lizards and snakes. BMC Evolutionary Biology 13:93.
- Rambaut, A. 2018. FigTree. Tree Figure Drawing Tool. Version 1.4.4 Available at http://tree.bio.ed.ac.uk/.Molecular Evolution, Phylogenetics and Epidemiology, University of Edinburgh, UK.
- Rambaut, A., A.J. Drummond, W. Xie, G. Baele, and M.A. Suchard. 2021. Tracer. MCMC Trace Analysis Tool, Version 1.7.2. Available at http://beast.community/tracer. Accessed on 10 November 2023. BEAST Developers, UK.
- Ramírez-Bautista, A. 1994. Manual y Claves Ilustradas de los Anfibios y Reptiles de la Región de Chamela, Jalisco, México. Cuadernos del Instituto de Biología 23. Universidad Nacional Autónoma de México, México.
- Rognes T., T. Flouri, B. Nichols, C. Quince, and F. Mahé. 2016. VSEARCH: A versatile open source tool for metagenomics. PeerJ 2016:e2584.
- Sabaj, M.H., 2023. Codes for Natural History Collections in Ichthyology and Herpetology (online supplement), Version 9.5. Available at https:// asih.org. American Society of Ichthyologists and Herpetologists, USA. Accessed on 10 November 2023.
- SEMARNAT (Secretaría de Medio Ambiente y Recursos Naturales). 2010. Norma Oficial Mexicana NOM-059-SEMARNAT-2010, Protección ambiental-Especies nativas de México de flora y fauna silvestres-Categorías de riesgo

- y especificaciones para su inclusión, exclusión o cambio-Lista de especies en riesgo. Diario Oficial de la Federación, 30 Diciembre 2010. Mexico.
- Smith, H.M. 1986. The generic allocation of two species of Mexican anguid lizards. Bulletin of the Maryland Herpetological Society 22:21–22.
- Smithe, F.B. 1975–1981. Naturalist's Color Guide. Part I. Color Guide. American Museum of Natural History, USA.
- Solís-Lemus, C., L.L. Knowles, and C. Ane. 2015. Bayesian species delimitation combining multiple genes and traits in a unified framework. Evolution 69:492–507.
- Stamatakis, A. 2014. RAxML Version 8: A tool for phylogenetic analysis and post-analysis of large phylogenies. Bioinformatics 30:1312–1313.
- Swofford, D.L. 2002. PAUP\*. Phylogenetic Analysis Using Parsimony (\*and Other Methods). Version 4.0a. Sinauer Associates, USA.
- Tihen, J.A. 1949. The genera of gerrhonotine lizards. American Midland Naturalist 41:579–601.
- Tihen, J.A. 1954. Gerrhonotine lizards recently added to the American Museum collection, with further revisions of the genus *Abronia*. American Museum Novitates 1687:1–26.
- Vázquez-Díaz, J., and G.E. Quintero-Díaz. 2007. Gerrhonotus liocephalus. The IUCN Red List of Threatened Species 2007: e.T63708A12707928. International Union for Conservation of Nature, Switzerland. Available at https://dx.doi.org/10.2305/IUCN.UK.2007.RLTS.T63708A12707928. en. Accessed on 17 June 2025.
- Wilson, L.D., V. Mata-Silva, and J.D. Johnson. 2013. A conservation reassessment of the reptiles of Mexico based on the EVS measure. Amphibian & Reptile Conservation 7:1–47.
- Woolrich-Piña, G.A., P. Ponce-Campos, J. Loc-Barragán, J.P. Ramírez-Silva, V. Mata-Silva, J.D. Johnson, E. García-Padilla, and L.D. Wilson. 2016. The herpetofauna of Nayarit, Mexico: Composition, distribution, and conservation status. Mesoamerican Herpetology 3:375–445.
- Yang, Z. 2015. The BPP program for species tree estimation and species delimitation. Current Zoology 61:854–865.
- Yang, Z., and B. Rannala. 2010. Bayesian species delimitation using multilocus sequence data. Proceedings of the National Academy of Sciences of the United States of America 107:9264–9269.

Accepted on 2 June 2025 ZooBank.org registration LSID: urn:lsid:zoobank.org:pub:5E27474D-D2F6-4435-8371-CACC478E7C8D

Published on 5 August 2025 Associate Editor: Christopher Raxworthy

#### APPENDIX

## Other Specimens Examined

Institutional abbreviations for museums and collections follow Sabaj (2023), except for MZFZ (Museo de Zoología of the Facultad de Estudios Superiores Zaragoza, Universidad Nacional Autónoma de México); ANMO and LNG numbers are field numbers for specimens to be catalogued in the MZFC-HE; EJV and RICB numbers are field numbers for specimens to be catalogued in the MZFZ.

Gerrhonotus liocephalus.—MEXICO: CHIAPAS: Cintalapa, Cerro Negrete (EJV21); Tonalá, Iglesia Vieja (LNG 1270). MÉXICO (STATE): Villa de Guerrero, Rancho el Tejocote (MZFC-HE 5030–31). GUERRERO: Eduardo Neri, Jalapa (RICB552–553); Zihuatanejo, Vallecitos de Zaragoza (MZFC-HE 20366). OAXACA: 3 km east of Guelatao (MZFC-HE 32957); road to Santa Maria Guienagati-Santiago Lachiguiri (MZFC-HE 16988, RICB533); Ramón Escobar Balboa (MZFC-HE 33389); Rodulfo Figueroa (MZFC-HE 33390); El Tejocote (UTA 6065, 19681, 22564, 22573, 30849); Huautla de Jiménez, Puerto de La Soledad (MZFC-HE 13233). PUEBLA: 1 mile north of Cacaloapan (UTA 4715); 4 km north of San Juan Tepanco (MZFC-HE 7829–30); Coxcatlán, Vigastepec (ANMO 4013–15); Tehuacán (RICB367).